Received: 8 July 2022 | Revised: 7 March 2023 | Accepted: 8 March 2023

DOI: 10.1002/hyp.14858

RESEARCH ARTICLE

WILEY

# Increasing fire frequency may trigger eco-hydrologic divergence

Shyanika Lakmali | Richard G. Benyon | Gary J. Sheridan | Patrick N. J. Lane

School of Ecosystem and Forest Sciences, Faculty of Science, Biosciences 1, The University of Melbourne, Parkville, Victoria, 3010, Australia

**Correspondence**
Shyanika Lakmali, Department of Plantation Management, Faculty of Agriculture and Plantation Management, Wayamba University of Sri Lanka, Makandura, Gonawila, Sri Lanka.
Email: lakmaliwas@wyb.ac.lk

**Funding information**
Victorian Department of Environment, Land, Water and Planning; Melbourne Water

## Abstract

Climate-induced fire regimes may change species abundance and species composition in affected forest types, potentially altering pyro-eco-hydrologic feedbacks. In some fire-prone forests across the globe, eco-hydrologic thresholds (changing points, or tipping points, in ecohydrology when vegetation shifts from one steady vegetation to another) are being exceeded due to changes in relationships between climate, fire and vegetation. Following compound disturbances, forests may fail to maintain ecological resilience. Under multiple burn conditions, *Eucalyptus regnans* F. Muell. forests in south east Australia are highly vulnerable to ecological tipping points. In Victoria, over 189 000 ha of obligate seeder forests have been burned two or more times within 18 years. These short return-interval fires allow *Acacia dealbata* to become the dominant overstorey species. Such a dramatic species replacement may result in a new evapotranspiration (ET) regime, leading to a new hydrologic state. Stand scale dynamic models were combined with field estimated ET in *E. regnans* and *A. dealbata* forests aged 10, 35 and 75/80 years. We found that long-term forest structure, ET and water yield significantly diverge between *E. regnans* and *A. dealbata* forests with increasing age. These divergences imply a non-equilibrium state after *A. dealbata* replaces *E. regnans* under high-frequency fire conditions. In senescing *A. dealbata*, understorey transpiration contribution of 29.8% to system ET was similar to that of overstorey transpiration (31.2%), indicating the understorey and overstorey contribute equally to total ET at the final stage of *Acacia* forests. In contrast, in 75-year-old *E. regnans* forests, understorey contribution to the total system evapotranspiration is about 16%. This suggests that, after the *Acacia* life cycle finishes, the ET regime will transit into a new state that will be dominated by shrubby understorey species. Our findings suggest that this climate-induced species replacement would decrease long-term ET, inferring an increase in streamflow.

**KEYWORDS**
climate-induced vegetation change, divergence in water yield, ecological tipping points, high-frequency fires, shift in ET regime

This is an open access article under the terms of the Creative Commons Attribution License, which permits use, distribution and reproduction in any medium, provided the original work is properly cited.
© 2023 The Authors. *Hydrological Processes* published by John Wiley & Sons Ltd.

## 1 | INTRODUCTION

In many vegetation types, disturbance history can be used as an indicator of long-term average fire return intervals, which are often more than 100 years (Murphy et al., 2013). Rapid climate change is altering these previously known disturbance regimes, which may, in turn, be altering mean evapotranspiration (ET) in some forest systems (Mirus et al., 2017; White & Jentsch, 2001). Usually, after a major disturbance, ecosystems recover to pre-disturbance status or begin a successional path that is reasonably well known or predictable. However, a sudden increase in disturbance frequency may trigger previously unseen, long-term changes to forest systems by causing loss of one or more key structural and functional attributes of the previous ecosystem (Buma et al., 2013). Such repeated disturbances may drive ecosystems towards a non-equilibrium state (Buma et al., 2013; Mori, 2011). Where a new forest type replaces the previously dominant forest, evapotranspiration (Et) may not equate to that of the pre-disturbance level if forest species mix and structure are significantly altered. Hydrologic responses to increased fire frequency may be complex or unexpected, and the longevity of those effects may be uncertain. For example, Niemeyer et al. (2020) found that annual stream flow increased after fire in all their study sites for a short term, as might be expected. However, in the one catchment that had not undergone any post-fire land management, recovery was unexpectedly slow, with streamflow remaining elevated for 35–41 years.

Climate-induced changes to fire regimes have been reported from many regions globally. For example, in the recorded US wildfire history, between 2014 and 2015, over 3.5 million hectares were burned by wildfires across Oregon, Washington, the western United States, conifer forests of the west side of the Cascade Range, and coastal temperate forests of the Olympic Peninsula (Halofsky et al., 2020). Over 10 million hectares burned during the summer of 2019/20, which was eastern Australia's worst fire season on record (Huf & Mclean, 2020). Further, short-interval fires also repeatedly burned forests in Mount Adams in southwestern Washington three times from 2008 to 2015 (Halofsky et al., 2020). The effect of this apparent increase in frequency and in intensity of wildfires on vegetation states and eco-hydrologic function is not well understood.

Australian native eucalypt forests are highly adapted to fire, and the vast majority of eucalypt species are fire-tolerant. Historic fire intervals range from a few years in dry foothill forests or savannah to around 100 years for the wet montane forests (Murphy et al., 2013). However, these forests have been subjected to the compound effects of climate change and fire regime shifts as the climate in Australia has become hotter and drier. These changes are triggering short-return-interval, high-intensity, mega-fire events. In south east Australia, ~2.6 million ha of forest was burned by three mega-fire events during the period of 2002–2009 (Fagg et al., 2013). In addition to these three mega-fire events (Figure 1a), medium and large-scale fires since 2003 have burned a considerable cumulative area of forest in Victoria (Fairman et al., 2016). Such climate-induced wildfires are

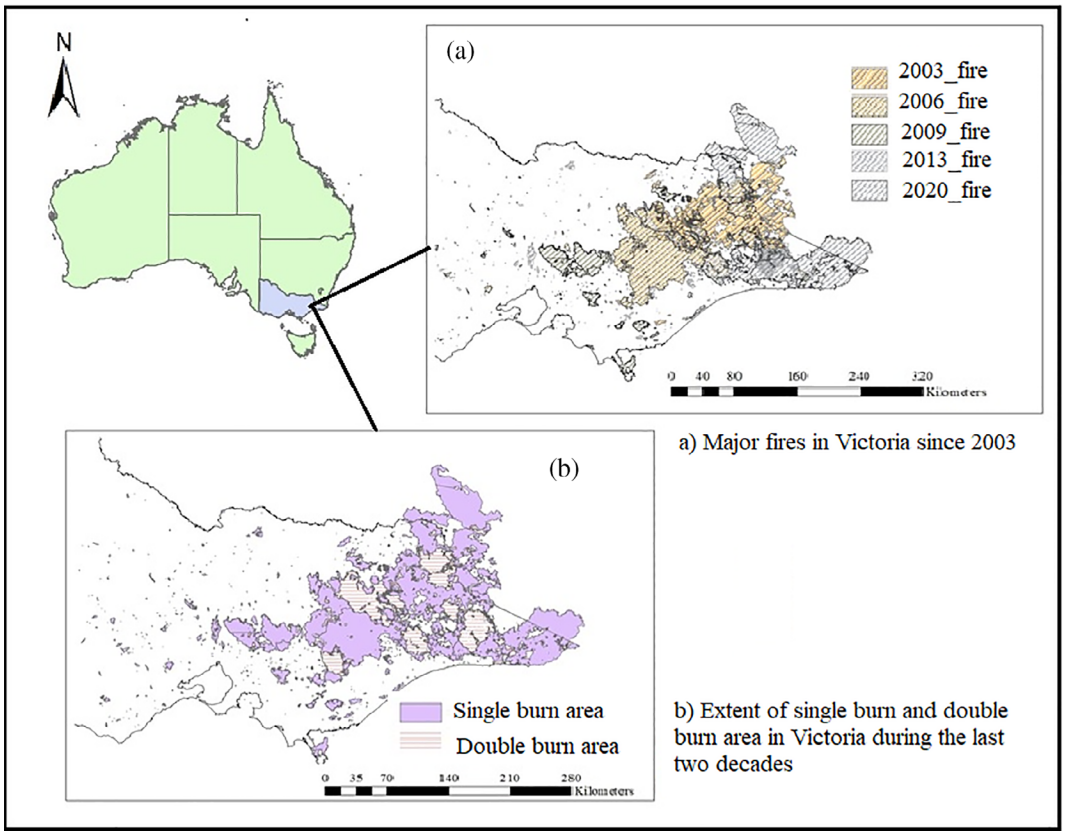



**FIGURE 1** (a) Major fires in Victoria since 2003 (extent of burned area in Victoria during major wildfires in 2003, 2006/07, 2009, 2013 and 2019/20). (b) Extent of single burn and double burn area in Victoria during the last two decades (2003, 2006/07, 2009, 2013 and 2019/20 fires).

unprecedented, unpredictable and are occurring at shorter time intervals, with modelling suggesting this trend will intensify (McColl-Gausden et al., 2022). As a result of this increased fire frequency, substantial areas of forest have been burned more than once since 2003 (Figure 1b), including some areas burned three times (Fairman et al., 2016). Despite their fire-adaptive traits, the more extreme, mainly climate-change-induced fire regimes experienced over the past two decades are a threat to eucalypt ecosystem stability (Bowman et al., 2014; Fairman et al., 2016). These climate-driven multiple fires in forests are resulting in significant changes to species abundance and species composition in many ecosystems (Buma et al., 2013).

Such changes suggest that even fire-adapted ecosystems have resilience thresholds that define the system's capability to tolerate multiple disturbance effects without switching into a structurally and functionally different state (Buma et al., 2013). Under multiple burns (within 15–20 years), ecosystems with historic fire return intervals of >100 years tend to exceed these ecological thresholds and shift to a qualitatively different state, indicating ecological tipping points have been reached (Bowman et al., 2014; Fletcher et al., 2013; Lindenmayer et al., 2011). Under multiple burns, the persistence of keystone species in southeast Australian forests are highly vulnerable. *Eucalyptus regnans* F. Muell. forests have keystone structural features (Lindenmayer, 2016). High-frequency fires may be creating a 'landscape trap' in *E. regnans* forests (Burns et al., 2015), which occurs when an entire forest is shifted into a new state and is then maintained as a structurally and functionally different state. Continuous changes to disturbance regimes can further shift ecological regimes, which may result in complete conversion from one species to another (Bowman et al., 2014, 2016). Past studies show that if multiple fires overlap in *E. regnans* forests in less than 20 years, regeneration may fail after the second fire due to less availability of seeds. Under such circumstances, understorey species such as *Acacia dealbata* Link can become the dominant overstorey species, leading to a broad-scale transition from *E. regnans* to *A. dealbata* or similar species. Long-lived (≈400 years) *E. regnans* is replaced with shorter-lived (80–90 years) *A. dealbata* (Bowman et al., 2014).

Such a broad-scale climate-induced species replacement clearly has significant ecological, and probably hydrological implications. Lakmali et al. (2022) found overstorey transpiration changed markedly over a chronosequence for these two species: as the stands aged, *A. dealbata* transpiration declined relative to that of *E. regnans*. While this demonstrates a fundamental eco-hydrologic change, it also has ramifications for streamflow dynamics. In this case, the potential impacts extend beyond the fundamentals of eco-hydrologic function. *E. regnans* (and another 'ash' species, *Eucalyptus delegatensis* R.T. Baker) are wet forests found mainly where mean annual precipitation is greater than 1200 mm in the headwaters of important stream systems. These 'ash' forests are the principal water source for Melbourne (population >4 million) and other towns. Previous studies have demonstrated a strong, and relatively unique, age-streamflow relationship in the ash forests (Kuczera, 1987; Vertessy et al., 2001), driven by their eco-hydrologic response to disturbance. Moderate or hotter fire results in high rates of mortality and single age regeneration, with younger forests exhibiting far higher water use than older stands. For example, annual ET of 1371 mm (76% of annual P) estimated at 15 years but only 911 mm (51% of annual P) at 240 years (Vertessy et al., 2001). This difference results in higher streamflow from older stands.

The impacts on eucalypt forest ecology and hydrology of a single wildfire in both ash (Brookhouse et al., 2013; Feikema et al., 2013; Haydon et al., 1996; Kuczera, 1987; Langford, 1976; Vertessy et al., 2001) and mixed species eucalypts (Gharun et al., 2013; Nolan et al., 2014, 2015); of logging (Bren et al., 2010; Hawthorne et al., 2013; Lane & Mackay, 2001; Watson et al., 2001; Webb et al., 2012); and of conversion to pasture or pine plantation (Bren & Hopmans, 2007; Ruprecht & Schofield, 1991) are well studied, with recovery trajectories reasonably well known. It should be noted that eucalypt recovery from fire is rapid compared with many other systems (see Niemeyer et al., 2020), with non-ash forests likely to recover biomass and hydrology within 5–10 years or even sooner (Gou et al., 2021; Khaledi et al., 2022; Nolan et al., 2015). However, hydrological responses to vegetation shift after multiple fires are largely unknown in the hydrological literature. Therefore, the primary intention of this study was to investigate the hydrological response of Melbourne's water supply catchments to multiple fires and vegetation shift. In this study, it was hypothesised that the replacement of *E. regnans* forests with *A. dealbata* forests would result in a significant decrease in annual and decadal ET, inferring an increase in catchment water yield. The main objectives of this study were, therefore to (i) quantifying the shift in ET regime in response to vegetation change that would result from multiple burns in native *E. regnans* forests; (ii) extrapolate from plot scale ET estimations to catchment scale for predicting the future streamflow trajectory if *A. dealbata* replaces *E. regnans* forest after multiple burns.

Intended outcomes of this study were achieved by examining the divergence in total ET between *E. regnans* and *A. dealbata* forests across an 80-year age sequence. Initially, key hydrological processes (annual ET components) were quantified (numerical quantity and partitioning between various processes differ from one species to another) and compared between these two forest types. Then, eco-hydrologic functions (functions representing ecological and hydrological conditions of the ecosystems) that explained differences in ET components between species were modelled, using measurable variables such as climate and forest structure, for predicting long-term ET trajectories in the two forest types. The aim was to provide comprehensive knowledge on how forest ET differs between *E. regnans* and *A. dealbata* forests over an entire life cycle, expanding our understanding of how streamflow will respond to climate-induced species replacement in future.

## 2 | MATERIALS AND METHODS

### 2.1 | Experimental design

A bottom-up, plot-based approach was used to estimate seasonal and annual ET and then these ET estimates were used to develop

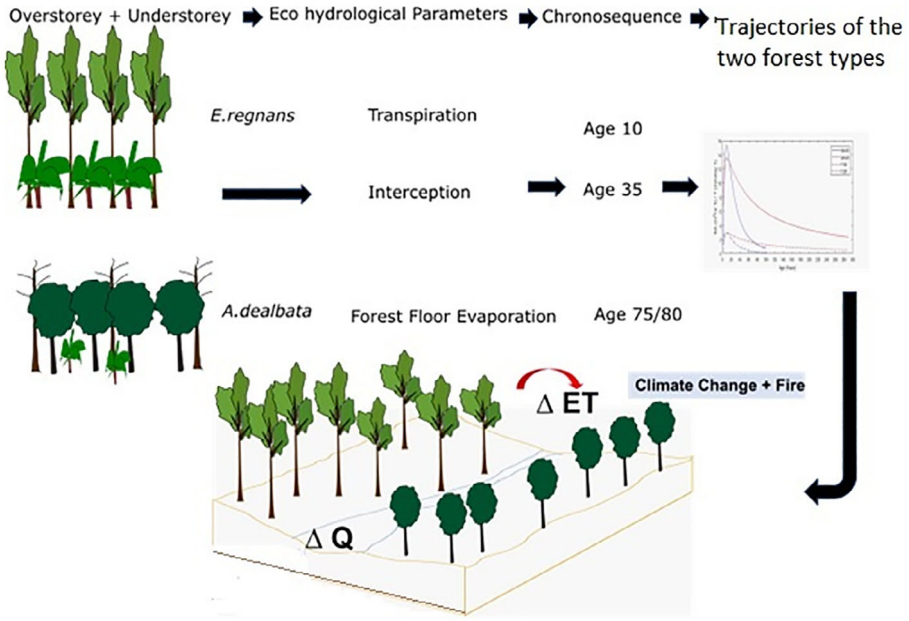



**FIGURE 2** Schematic diagram for a conceptual model for experimentation.

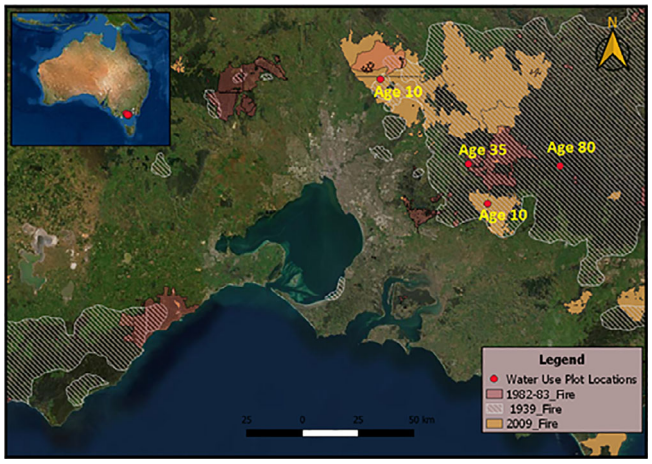



**FIGURE 3** Selected study locations. In each age group, adjacent *Eucalyptus regnans* and *Acacia dealbata* forests were selected for measuring eco-hydrologic parameters, except in the 80-year-old where only *A. dealbata* was present.

empirical models of the long-term hydrological response of forested water catchments to vegetation change. The conceptual model that was adopted during the present study is illustrated in Figure 2. ET components were compared between *E. regnans* and *A. dealbata* at various stages in the life cycles of these two forest types in representative plots at the locations shown in Figure 3. Each location included paired plots of both species except for the 80-year-old where the two plots were both *A. dealbata*. Field-based, half-hourly to monthly measurements of the various components of ET were taken from these plots and supplemented with additional data from similar plot-scale measurements by Benyon et al. (2017), who measured all components of ET in *E. regnans* aged 75 years and by Hawthorne et al. (2018), who measured overstorey transpiration in both species in a mixed stand aged 20 years. Some additional data on understorey transpiration rates per unit of leaf area and on ET from older *E. regnans* from Vertessy et al. (1998) were used for estimating long-term ET trajectories (see Section 2.8.3).

Remoteness of the field sites and limitations on time and resources meant that not all components of ET could be measured accurately at all sites. Further, theft of equipment meant that measurements ended prematurely at the wetter 10-year-old site (southern-most in Figure 3, referred to here as 'Bunyip Road') after only 5 months. The most comprehensive measurements were collected from mid-spring to late summer (October to February), but at some sites measurements of overstorey transpiration and interception were collected for a year or more (the 10-year-old, northern plots at 'Wallaby Creek', 80-year-old *A. dealbata* at 'Toorongo Road' and 75-year-old *E. regnans* by Benyon et al. (2017)).

Measurements and comparisons of overstorey sap velocities and transpiration of the two species over the age sequence have been reported in detail in Lakmali et al. (2022). This paper focuses on measurements of the other components of ET (interception and ET from forest floor) and on the derivation of long-term ET and streamflow trajectories for the two species.

As detailed in Lakmali et al. (2022), the sites shown in Figure 3 were selected from pure stands of *E. regnans* and *A. dealbata*, regenerated after high severity fires. Pure 80-year-old *A. dealbata* stands on the Toorongo Plateau replaced *E. regnans* forest following successive fires in 1926 and 1939. All of the other *A. dealbata* forests were regenerated as pure patches of Acacia after single high-intensity fires in 1983 ('Britannia Creek' plots, aged 35) or 2009 ('Wallaby Creek' and 'Bunyip Road' plots, aged 10). It is not clear why these stands exist in a pure form, but they mimic the 'double burn' response.

Field observations indicated *A. dealbata* forests can live for little more than 80 years. During site selection, in ~70% of the 80-year-old *A. dealbata* stands visited, most or all of the *Acacia* overstorey trees were already dead. However, in some *Acacia* stands, the *Acacia*

overstorey was still alive. To enable confirmation of the differences in ET between the two species at age 75/80, only *A. dealbata* stands with live overstorey were selected for measuring eco-hydrologic parameters. However, these live stands were not representative of the majority of stands with close to 100% mortality at age 80. Apart from the above stands, ~75-year-old *E. regnans* forests (1939 regrowth) studied by Benyon et al. (2017, Plots 2 and 3) were used to complete the comparison in ET between the two species within the ~80-year life cycle of *A. dealbata* forests.

## 2.2 | Plot-scale ET estimation in the two forest types across the chronosequence

Transpiration, interception and evaporation from the forest floor were measured where practical in the understorey vegetation to complete total ET estimations in the water use plots. Total ET was calculated, as shown in Equation (1). The data were collected in most of the plots covering nearly a year, but data were selected from October to February (the common data collection period to all stands) to enable direct comparison between the two forest types (Table S1).

$$\mathrm{ET} = [T + I]_{\mathrm{OS}} + [T + I + \mathrm{EVP}]_{\mathrm{US}}, \quad (1)$$

where, $T$ is transpiration, $I$ is interception, EVP is forest floor evaporation, OS denotes overstorey and US denotes understorey.

## 2.3 | Overstorey transpiration

Overstorey sap velocity and transpiration measurements used in the present study have recently been reported in Lakmali et al. (2022). Readers are referred to that publication for details of the methods used and results. Here we present a summary and explain how these measurements were combined with observations from earlier studies (Benyon et al., 2017; Hawthorne et al., 2018; Vertessy et al., 1998) to derive long-term overstorey transpiration trajectories for both species.

### 2.3.1 | Overstorey mean sap velocity

Before Hawthorne et al. (2018) and Lakmali et al. (2022), sap velocity and transpiration were measured in *E. regnans* overstorey in various studies (Benyon et al., 2017; Dunn & Connor, 1993; Vertessy et al., 2001) but almost exclusively only in the mature to senescing growth stages (overstorey aged ~50, ~75, ~90, ~150 and ~230-years-old). Hawthorne et al. (2018) measured sap velocities and transpiration for almost 6 months (October to March) in a mixed stand of 20-year-old *E. regnans* and *A. dealbata*. To enable comparison of mean sap velocity and overstorey transpiration between the two species across the ~80-year life cycle of *A. dealbata*, Lakmali et al. (2022) collected sap velocity measurements from the eight paired water use plots at the locations shown in Figure 3.

The Lakmali et al. (2022) sap velocity measurements were made in 5–8 trees per plot using the heat ratio method. Sap velocity of each sample tree was corrected for thermal diffusivity (Marshall, 1958), wounding (Burgess et al., 2001), and for zero baseline offset. Tree level sap flux density (sap flow volume per unit of sapwood area per unit of time) was up-scaled to stand transpiration by multiplying stand mean sap flux density by overstorey mean sapwood area of each species/age class measured in the 35 inventory plots (see Lakmali et al., 2022, supplementary material). As detailed in Lakmali et al. (2022), measurements were made for different periods (5–15 months) and in different years between February 2017 and January 2019. Their analysis comparing mean sap velocities between age classes and species included correction for differences in climatic conditions between sites and years (see figs. 3 and 4 and tab. 3 in Lakmali et al., 2022). Their conclusions, in agreement with earlier studies in *E. regnans*, was that when averaged over periods of months to a year, mean sap velocity in both species is largely independent of age. This enables overstorey annual transpiration in both species to be predicted as a function of sapwood area.

### 2.3.2 | Overstorey sapwood areas

Overstorey sapwood area has been shown to be the most important determinant of long-term transpiration trends in these two forest types. Dunn and Connor (1993) and Vertessy et al. (2001) showed that mean sap velocity in *E. regnans* overstorey was independent of age, while Benyon et al. (2017) observed that mean sap velocity did not vary significantly spatially within the 75-year-old *E. regnans* age class and concluded that the main determinant of both temporal and spatial variation in stand annual transpiration in *E. regnans* is sapwood area. Lakmali et al. (2022) extended this analysis to include *A. dealbata* and showed that in this species, stand sapwood area is also the main determinant of variation in annual transpiration both in space and time.

A forest inventory survey was conducted to quantify structural trajectories, including stand mean dbh, stand basal area and stand sapwood area in the two forest types (Lakmali et al., 2022). This included the 11 forest patches used for water use measurements (Benyon et al., 2017; Hawthorne et al., 2018; Lakmali et al., 2022) and another 35 inventory plots (Lakmali et al., 2022) used for stand basal area and stand sapwood area estimations in eight species/age class combinations (Table S2). In all water use and inventory plots, bark thickness and sapwood thickness were measured in two to six cores per tree. In *E. regnans*, heartwood was detected by staining with 1% Methyl-Orange solution, while in *A. dealbata* the heartwood is distinctly darker than the sapwood. Tree sapwood area at breast height was estimated using the mean sapwood thickness and under-bark stem diameter measurements. A linear regression relationship between tree basal area and tree sapwood area was used to predict sapwood area for ~20% of smaller trees in which sapwood thickness was not

measured (Lakmali et al., 2022). Stand sapwood area for each inventory plot in each species/age class was estimated as the sum of the sapwood areas of the individual trees, expressed in $m^2$ $ha^{-1}$. The stand basal area of each plot was estimated as the sum of the individual tree basal areas, expressed in $m^2$ $ha^{-1}$.

## 2.4 | Throughfall, stem flow and canopy interception

Previously, Haydon et al. (1996) reported that mean interception percentage varies with overstorey age in *E. regnans*. For the present study, variation in mean interception percentage between *E. regnans* and *A. dealbata* forests with age was estimated using both throughfall and stem flow measurements in each species/age class (the same plots used for the sap velocity measurements reported in Lakmali et al., 2022), except for the Hawthorne et al. (2018) 20-year-old plots. Interception (*I*) in each plot was estimated using Equation (2).

$$I = P - \mathrm{TF} - S, \tag{2}$$

where, TF is throughfall, *P* is incident precipitation, *S* is stem flow.

Throughfall in each plot was measured monthly using six to eight V-shaped 1.2 m × 0.14 m steel gutters per plot, as described in Benyon et al. (2017). When understorey was present (both species aged 35 and 75/80 years), understorey interception was estimated by placing four throughfall collectors beneath the understorey and four beneath overstorey only.

Monthly stem flow was also measured in four overstorey trees per plot in each of the Lakmali et al. (2022) water use plots, using stem flow collars draining into collectors. Stem flow on an area basis in mm, was estimated as the product of stem flow collected per tree and tree density. Monthly interception was estimated as the sum of monthly stem flow and throughfall subtracted from monthly precipitation measured in clearings near each site (see Lakmali et al., 2022 for weather station locations).

## 2.5 | Transpiration and leaf area index in woody understorey

### 2.5.1 | Understorey transpiration

Most of the water use plots had either no understorey (all of the 10-year-old plots) or an understorey composed of ferns, other non-woody vegetation and small shrubs. Only in one 80-year-old *A. dealbata* plot ($TR_4$) was there woody understorey with stems large enough (up to 10 cm DBH) to permit sap flow measurement. In this plot, sap velocities were measured in a sample of six stems between 25 October 2018 and 14 January 2019 using the same method as for the overstorey. As there was no identifiable heartwood in these shrubs, understorey daily transpiration was estimated as the product of daily mean sap velocity and woody understorey total basal area under bark measured in eight 3 m diameter sub-plots. In the other water use plots with small ferns and shrubs, transpiration of some small understorey plants was measured as part of forest floor evaporation as described in Section 2.6, but this did not include transpiration from larger understorey ferns and shrubs. Understorey ET components measured by Benyon et al. (2017) were used to complete total ET estimates in 75-year-old *E. regnans*.

### 2.5.2 | Understorey leaf area index

Our measurements of understorey transpiration were limited and confined to only a short period of the year. In the one plot where we were able to use sap flow sensors in the understorey, our inability to identify heartwood may have resulted in over-estimation of understorey transpiration. As an alternative, we used a combination of understorey transpiration rates per unit of leaf area measured by Vertessy et al. (1998) with our own measurements of understorey leaf area index (LAI) in our water use plots (Lakmali, unpublished PhD thesis), to derive estimates of annual understorey transpiration for various ages (see Section 2.8.3).

As detailed in Lakmali et al. (2022), hemispherical images were used to estimate LAI in each of the water use plots. Understorey LAI was estimated by calculating the difference between measured total LAI and overstory LAI in the plot. From each plot, 20–25 images were collected during different seasons to calculate average LAI for each species age class. Hemispherical canopy photo images were taken with a Nikon Coolpix 8400 digital camera, equipped with an FC 8 mm fisheye lens. Image acquisition was made before sunrise or under overcast conditions to avoid direct sunlight, which may cause errors in LAI estimation (Welles & Norman, 1991). The camera was mounted facing upwards on a self-levelling tripod and aligned to magnetic north at the time of image acquisition. The exposure of the camera was calibrated at each LAI measurement plot as described by Macfarlane et al. (2007). All hemispherical images were analysed using the Hemi view 2.1 (Delta-T devices, Ltd., Cambridge, UK) image processing software package.

## 2.6 | ET from the forest floor and non-woody understorey

ET from the forest floor, including transpiration from small, non-woody understorey plants (<0.7 m tall) was measured in each species/age class using an evaporation chamber method described in detail by Mitchell et al. (2012). Over 3–6 days in each of the 10-year-old and 35-year-old plots, between September 2018 and February 2019 (spring and summer), instantaneous soil evaporation was measured in three to five consecutive runs. Each run consisted of six random sampling points inside the plot for which the evaporation rate was measured for a period of 1 min. Measurement dates and number of runs on each day in each plot are listed in Table S3. The 1 m high × 0.7 m diameter chamber was placed on the forest floor and the fan was

started at low speed to ensure air in the chamber was mixed well while collecting measurements. Variations in temperature and humidity inside the chamber were recorded by sensors every second for 1 min. Data were saved in a small tablet connected to the sensors. The recorded changes in moisture content of the air inside the chamber during the 1-min sampling period were used to calculate the evaporation rate during that period in mm $s^{-1}$ as described by Ward and Micin (2006). These point data were then averaged across all points, runs and days for each plot to derive estimates of plot mean evaporation rates.

## 2.7 | Species and age effect on total ET and ET components

Monthly ET for each plot for the October to February period was calculated using Equation (1) and differences in monthly ET between the two forest types across the age classes were tested with a two-factor repeated measure analysis of variance (ANOVA). Multiple comparisons across species and age were undertaken with Tukey's HSD post hoc test.

## 2.8 | Determining long-term ET trajectories for the two forest types

This section describes how long-term ET trajectories were developed for each species using a combination of ET data collected for this study and previously published estimates of various ET components for *E. regnans*.

As noted in Section 2.1, at age 80 in some acacia stands, the acacia overstorey was still alive, but in other stands, most or all of the acacias were dead. Due to the fact that we selected live stands, the plot-scale measurements gave a biased estimate of overstorey ET for 80-year-old *A. dealbata* stands as they did not account for likely much lower overstorey ET of 80-year-old stands in which the acacia overstorey had recently died. To account for this, two total ET trajectories were developed for the acacias: one for stands in which the acacia overstorey is still alive at age 80 and another assuming a gradual decline in sapwood area after age 35 to near zero at age 80 in accordance with the measured data for age classes in the field survey.

Long-term overstorey ET versus age relationships for the two forest types were developed using a method similar to that of Haydon et al. (1996). Long-term annual trajectories of overstorey transpiration (Section 2.8.1), interception (Section 2.8.2) and understorey ET (Section 2.8.3) were combined to estimate long-term total ET for the two forest types. For *E. regnans*, a generalized ET trajectory was developed up to age 240 years to illustrate what happens in this species beyond the age of 80 years. For *A. dealbata*, two total ET trajectories were derived based on the status of the overstorey contribution to system ET as discussed above: one for stands in which the acacia overstorey was still alive at age 80 and another assuming a gradual decline in sapwood area to near zero at age 80.

### 2.8.1 | Determining long-term overstorey transpiration trajectories of the two forest types

Benyon et al. (2017) confirmed earlier findings that in *E. regnans*, mean annual sap velocity is not significantly influenced by stand age (Dunn & Connor, 1993; Vertessy et al., 2001) and does not vary between sites when there is no water limitation on sap velocity. Similarly, Lakmali et al. (2022) found no difference among mean sap velocities in *A. dealbata* at ages 10, 35 and 80 (was lower in Acacia at age 20) using non-water limited sap flow measurements from different sites and age classes in *A. dealbata*. Therefore, a single annual sap flux density can be used to calculate overstorey annual transpiration in each forest type across all age classes. Similar to Haydon et al. (1996), species-specific annual overstorey transpiration trajectories for the two forest types were developed, using a sapwood area versus age model in Equation (3).

$$T_{os} = K \times SA_j, \tag{3}$$

where, for each species, $T_{os}$ is annual transpiration of the overstorey at age $j$; $K$ is the species-specific value for annual sap flux (transpiration) per $m^2$ of sapwood area used for all ages. In this study $K$ for *E. regnans* and *A. dealbata* forests are 788.4 and 693.8 $m^3\ m^{-2}\ yr^{-1}$, respectively, derived from full-year measurements in the 10-year-old stands at Wallaby Creek, the 80 year old *A. dealbata* stands at Toorongo Road (Lakmali et al., 2022) and the 75-year-old *E. regnans* stands reported by Benyon et al. (2017); $SA_j$ is sapwood area at age $j$, estimated using an age-driven sapwood area model for each species.

Age-driven, empirical sapwood area models were developed for both species by combining plot-based measurements of stand sapwood area collected for this study (Lakmali et al., 2022) with additional data from the literature (Benyon et al., 2015, 2017; Hawthorne et al., 2018). Curve fitting and parameter estimation were done using 'MATLAB®' mathematical software. Models were separately fitted to the measured sapwood areas in the two forest types across different ages. The best two models were selected for sapwood area estimation in the two forest types based on the goodness of fit criteria (Table 1).

To account for the two alternative acacia stand types (overstorey alive and overstorey dead at age 80), the overstorey transpiration trajectory for *A. dealbata* forests was established with upper and lower boundaries in-between age 35 and 80. A lower overstorey transpiration trajectory was developed by assuming a gradual decline in the sapwood area of *Acacia* overstorey to near zero at age 80. An upper trajectory was determined by considering only *A. dealbata* forests in which the overstorey was still alive. For *E. regnans* forests, the most generalized overstorey transpiration trajectory was developed by considering the most representative sapwood area versus age curve for the entire life span, derived from measurements of stand sapwood area collected in the present study and by Benyon et al. (2017) for stands aged up to 75 years and from Vertessy et al. (1998) for stands aged 120 and 240 years.

**TABLE 1** Estimated parameters for stand sapwood area (SA) models for *Acacia dealbata* and *Eucalyptus regnans* forests.

| Species | SA model structure | Parameters | Goodness of fit |
|---|---|---|---|
| *A. dealbata* | $\beta_0 \times \exp(-0.5(\ln(\text{Age}/\beta_1)/\beta_2)^2)$ | $\beta_0 = 15.34$ | SSE: 417.3 |
| | | $\beta_1 = 9$ | $R^2$: 0.61 |
| | | $\beta_2 = 0.979$ | $R^2$-adj: 0.58 |
| | | | RMSE: 3.669 |
| *E. regnans* | $\beta_0 \times \exp(-0.5(\ln(\text{Age}/\beta_1)/\beta_2)^2)$ | $\beta_0 = 13.49$ | SSE: 182.1 |
| | | $\beta_1 = 9$ | $R^2$: 0.68 |
| | | $\beta_2 = 1.857$ | $R^2$-adj: 0.66 |
| | | | RMSE: 2.423 |

**TABLE 2** Understorey ET components and sources used for estimating the annual understorey ET trend of the two forest types, assuming annual rainfall of 1800 mm.

| Species/age class | LAI ($m^2\ m^{-1}$) | Transpiration (mm $year^{-1}$) | Interception (mm $year^{-1}$) | Evaporation (mm $year^{-1}$) | Total ET (mm) |
|---|---|---|---|---|---|
| *A. dealbata* | | | | | |
| 10 | 0 | 0 | 0 | 95[a] | 95 |
| 35 | 0.20 | 25[b] | 57.6[a] | 94.5[a] | 177.1 |
| 80 | 1.15 | 145[b] | 252[a] | 100.7[a] | 497.7 |
| *E. regnans* | | | | | |
| 10 | 0 | 0 | 0 | 91[a] | 91 |
| 35 | 0.40 | 50.4[b] | 90[a] | 94.9[a] | 235.3 |
| 75 | n.m. | 232.8[c] | 126[a] | 117[a] | 475.8 |
| 120 | n.m. | 290[c] | 139.7[d] | 110[c] | 539.7 |
| 240 | n.m. | 300[c] | 145.46[d] | 100[c] | 545.5 |

Abbreviation: n.m., not measured.
[a]Interception measured in our plots (Section 2.4) and soil evaporation (Section 2.6).
[b]LAI from the present study (Lakmali et al., 2022) multiplied by T/LAI from Vertessy et al. (1998), tab. 6 notes.
[c]Directly from Vertessy et al. (1998), tab. 6.
[d]Using sapwood area from Vertessy et al. (1998) tab. 6 in the relationships between sapwood area and total and overstorey interception from fig. 6 in Benyon et al. (2017).

### 2.8.2 | Determining long-term variation in canopy interception with forest age

Previous studies have derived LAI versus age trajectories using mathematical functions for the different forest types (Nolan et al., 2015; Watson, 1998). Statistically significant relationships between LAI and canopy storage capacity have been reported in De Jong and Jetten (2007) and Van Dijk and Bruijnzeel (2001), implying the interception rate is controlled by LAI. Ghimire et al. (2017) stated that interception losses are shown to be related to forest age, which implies age-related changes in LAI control interception loss in forests over their lifetime. Given that interception is determined by LAI, in forests where LAI varies with age, interception should also be a function of age. Therefore, the curve shape for canopy interception variation over time was determined using the basic model structure developed by Watson (1998). Total interception versus age curve was fitted for each species based on measured data for the two forest types as described by Watson (1998) and Nolan et al. (2015). Long-term interception rates for *E. regnans* forests published in the literature (Haydon et al., 1996) were compared with the interception trajectory of *E. regnans* forest derived in the present study.

### 2.8.3 | Annual estimations of understorey ET

For each forest type and age class, annual total understorey ET was calculated by summing various estimates of understorey transpiration, interception and forest floor evaporation collected as part of this study or derived from the literature (Table 2). As noted previously, in the 10-year-old stands, there was no understorey and therefore no understorey transpiration or interception. In the 35-year-old forests, understorey transpiration was not measured due to resource and time limitations. The limited measurements of understorey transpiration in the 75/80-year old-stands had a high degree of uncertainty associated with them. For the 75-year-old stand in which understorey transpiration was measured by Benyon et al. (2017) the understorey was only 4 years old at the time of measurements, having regenerated following low-intensity fire 4 years earlier, and so was not representative of 75-year-old understorey. The most consistent and reliable

approach to estimating understorey transpiration in 35 and 75-year-old *E. regnans* was to multiply an understorey transpiration rate per unit of leaf area published in the notes to table 6 of Vertessy et al. (1998) by understorey LAI measured in the present study. To use the same method for our 35 and 80-year-old *A. dealbata* it was necessary to assume that the understorey transpiration rate per unit of leaf area from Vertessy et al. (1998) does not change between overstorey species. Vertessy et al. (1998) used measurements of understorey transpiration and LAI in *Pomaderis aspera* and *A. dealbata* and their 55- and 15-year-old *E. regnans* overstoreys to derive understorey transpiration estimates of 126 mm year$^{-1}$ per unit of understorey LAI. As the understorey transpiration rates are likely to be determined by shading from overstorey LAI irrespective of overstorey species, we hypothesise that this rate will be independent of overstorey species.

Our objective was to compare ET trajectories between *A. dealbata* and *E. regnans* forests during their full life spans, or as close as possible. The life cycle length in *E. regnans* can be up to 400 years (Ashton, 1981), but at the present time there are no stands in Victoria that exceed 250 years, whereas *A. dealbata* forests life cycle limit at 80 years. Table 2 includes two extra age classes of *E. regnans*, representing ET of *E. regnans* forests in the oldest age classes in which it has been measured and is representative of this species in the later stages of its life cycle. ET components of old-growth *E. regnans* forests are well studied and published in the literature. Therefore, ET estimation of this study was extended for *E. regnans* to develop ET and streamflow trajectories that represent the later part of its lifecycle. As with interception, understorey annual ET versus age curves were fitted for each species using the estimates for the various ages from Table 2.

## 2.9 | Catchment-scale approximation and long-term water yield prediction

As mentioned in Section 2.8.1, the measured sapwood areas were used to estimate long-term trends of forest sapwood area in the two forest types over their life cycles. These two models were approximated to the catchment scale, to give $SA_j$ in Equation (3), as follows. A sapwood area/age model developed by Haydon et al. (1996) was used to estimate a catchment-scale sapwood area versus age relationship for *E. regnans* forests. The Haydon et al. (1996) model was preferred for this because our measurements were confined to fully stocked pure stands whereas the Haydon et al. model was based on randomly selected plots that included poorly stocked parts of their study catchments that occurs due to variable (patchy) regeneration density, so is probably more representative of whole catchments. A catchment-scale adjustment for the *A. dealbata* forests was made by assuming that at the catchment scale *A. dealbata* regeneration would be similarly patchy and proportionately adjusting the *Acacia* sapwood area curve using the ratio between the sapwood area of Haydon et al. (1996) and sapwood area estimated for *E. regnans* forests during the present study throughout the chronosequence (Equation 4).

$$\text{adjusted sapwood area}\,(A.\,dealbata) = \frac{SA\,ER_1}{SA\,ER_2} \times SA\,AD_2, \quad (4)$$

where, adjusted sapwood area (*A. dealbata*) = sapwood area of *A. dealbata* adjusted to catchment scale, SA $ER_1$ = sapwood area predicted by Haydon et al. (1996) for *E. regnans*, SA $ER_2$ = sapwood area predicted in the present study for *E. regnans*, SA $AD_2$ = sapwood area predicted in the present study for *A. dealbata*.

The adjusted sapwood area versus age relationships (Haydon et al. relationship for *E. regnans* and adjusted *A. dealbata* relationship for *A. dealbata*) were applied in Equation (3) for ages 1–80 years for *A. dealbata* and ages 1–240 years for *E. regnans* to develop catchment-scale transpiration versus age relationship for each species.

Annual overstorey interception across these age ranges, calculated using a mean annual precipitation of 1800 mm (the same as Vertessy et al., 1998, 2001) and the percentage interception versus age relationships developed in Section 2.8.2 was added to overstorey transpiration. Finally, understorey ET versus age, as described in Section 2.8.3 was added to overstorey transpiration and total interception estimated for each age to give total ET versus age relationships for each species up to age 80 for *A. dealbata* and to age 240 for *E. regnans*.

Streamflow trajectories throughout their lifetime in *E. regnans* and *A. dealbata* forests were determined by subtracting the catchment-scale annual ET versus age estimates as described above from the mean annual precipitation of 1800 mm.

# 3 | RESULTS

## 3.1 | Comparison of ET between *Eucalyptus regnans* and *Acacia dealbata* forests

Species and age had a significant effect on overstorey ET (the sum of overstorey interception and transpiration) and total ET (the sum of overstorey and understorey ET). The field measured overstorey ET, from October to February, showed that, at age 10, over storey ET was 8% higher in *A. dealbata* ($p < 0.05$, Table 3). However, from age 35 onwards, overstorey ET rates were significantly higher in *E. regnans* ($p < 0.001$, Table 3) compared to *A. dealbata*. Total ET did not reduce systematically with forest age (Figure 4b) because the understorey contribution to total ET increased between ages 35 and 80, especially in *A. dealbata*.

In *A. dealbata*, total ET was higher in the 80-year-old forest than in 35-year-old forest (Figure 4b) because of a higher contribution of both understorey transpiration (Figure 5) and understorey interception to total ET.

However, the total ET in 80-year-old *A. dealbata* forests was still lower than that of similar-aged *E. regnans* forest (Figure 4b). Accordingly, in *A. dealbata* forests, daily total ET over late spring and summer (October–February) was 3.3 mm day$^{-1}$ compared to 3.7 mm day$^{-1}$ for the same period of the year in similar-aged

| Two-factor repeated measures of ANOVA | | | Multiple comparison (*p*-value) |
|---|---|---|---|
| **Component** | **Effect** | ***p*-value** | ***E. regnans* versus *A. dealbata*** |
| Overstorey evapotranspiration | Species | 0.015* | |
| | Age | 9.06e−10*** | |
| | Age 10 | | 0.0345* |
| | Age 35 | | 4.49e−06*** |
| | Age 80 | | 1.25e−06*** |

*Note*: *p* values for post hoc tests are reported for multiple comparisons. Significant levels: 0.05*, 0.01**, 0.001***.

**TABLE 3** Summary of two-factor repeated measures of ANOVA for mean monthly overstorey ET for *Eucalyptus regnans* and *Acacia dealbata* forests across the age sequence that was measured over the October to February period.

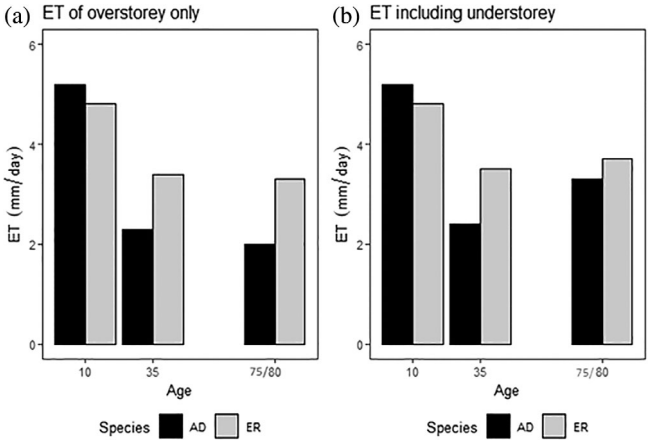



**FIGURE 4** Overstorey ET (overstorey transpiration + overstorey interception) and total ET in the two forest systems at ages 10, 35 and 75/80 years for the October to February period (a) overstorey only and (b) both overstorey and understorey.

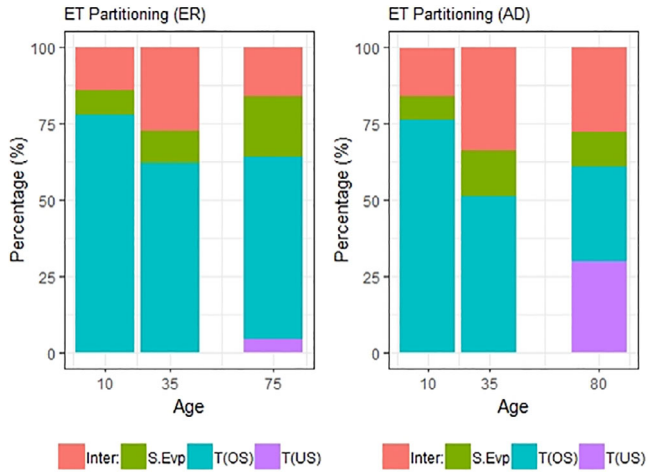



**FIGURE 5** ET partitioning in *Eucalyptus regnans* and *Acacia dealbata* forests with age (Inter: – overstorey and understorey interception, S. Evp – forest floor evaporation, T(OS) – overstorey transpiration, T(US) – understorey transpiration).

*E. regnans*. Further, results suggest that by age 80, understorey contribution to total ET was about 40% in *A. dealbata* but only about 30% in *E. regnans*, indicating that the understorey contribution to the system water balance was significantly higher in *A. dealbata* forests in their senescing stage.

## 3.2 | ET partitioning between *Eucalyptus regnans* and *Acacia dealbata* forests

In both forest types, overstorey transpiration was the largest component of total ET, but its proportional contribution reduced with forest age (Figure 5). In *A. dealbata* forests, the contribution of overstorey transpiration reduced rapidly from 76% at age 10 to 31% at age 80 whereas, in *E. regnans* forests, it declined from 77% to 59%. Interception was the second largest component flux of total ET. At ages 10 and 35, the contribution of total interception to total ET was only slightly higher in *A. dealbata* than in *E. regnans*, but at age 80 it was substantially higher (Figure 5). Total interception accounted for 28% of ET in 80-year-old *A. dealbata* forests but only 16% of ET in similar-aged *E. regnans* forests.

## 3.3 | Long-term divergence in forest structure between the two forest types

Structural differences between *E. regnans* and *A. dealbata* forests become apparent with stand age as shown in Figure 6. Variation of stand mean dbh and stand basal area along the chronosequence between the two forest types reflects the dramatic divergence in forest structure between *E. regnans* and *A. dealbata* forests that has begun by age 20 years (Figure 6). This divergence continues until the end of the life cycle of the shorter-lived *Acacia*.

In *A. dealbata* forests, sapwood area declines rapidly after age 20 throughout the rest of their life. In contrast, forest sapwood area in *E. regnans* reduces slowly over their (much longer) lifetime.

## 3.4 | Long-term overstorey transpiration trajectories of the two forest types

Long-term overstorey annual transpiration trajectories for the two forest types are presented in Figure 7. The upper line for *A. dealbata* in Figure 7 indicates the trajectory when the *A. dealbata* overstorey is

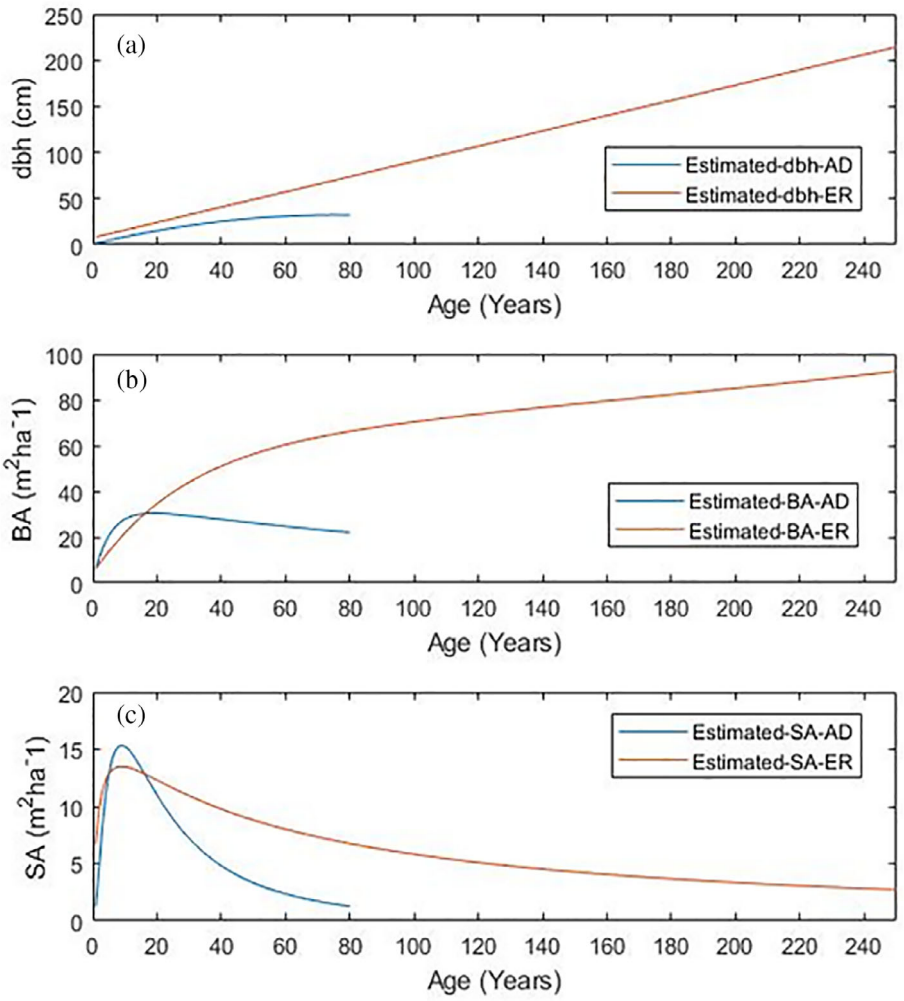



**FIGURE 6** Divergence in stand mean dbh (a), stand basal area (b) and overstorey stand sapwood area (c) between *Eucalyptus regnans* and *Acacia dealbata* over the age sequence.

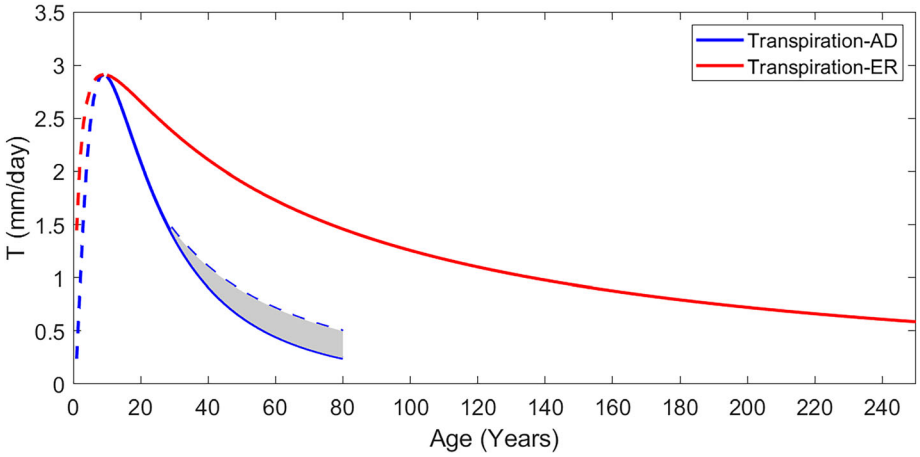



**FIGURE 7** The hypothesised overstorey transpiration ($T_{os}$) trajectories for *Acacia dealbata* and *Eucalyptus regnans* forests. For *A. dealbata*, the upper line indicates the trajectory for stands in which the *A. dealbata* overstorey is still alive at age 80. The lower line assumes a gradual decline in overstorey sapwood area to near zero at age 80.

still alive at age 80, while the lower curve is the trajectory assumed to occur if sapwood area declines gradually to near-zero at age 80 due to death of the *A. dealbata* overstorey. Across all *A. dealbata* stands, the mean trajectory is likely to be somewhere in the shaded area between the two lines.

In all transpiration trajectories, the peak $T_{os}$ of the two forest types occurs around age 10. The models predict a sharp decline of $T_{os}$ in *A. dealbata* forests from about 2.8 mm day$^{-1}$ at age 10 to 0.2 mm day$^{-1}$ by age 80 if most of the overstorey trees are dead or to 0.7 mm day$^{-1}$ for stands where the overstorey is still alive. For both trajectories, the overstorey contribution of *A. dealbata* forests to the total system ET declines sharply with forest age. Overstorey transpiration in *E. regnans* forests declines more gradually from 2.8 mm day$^{-1}$ at age 10 to 1.5 mm day$^{-1}$ at age 75. From 10 years of

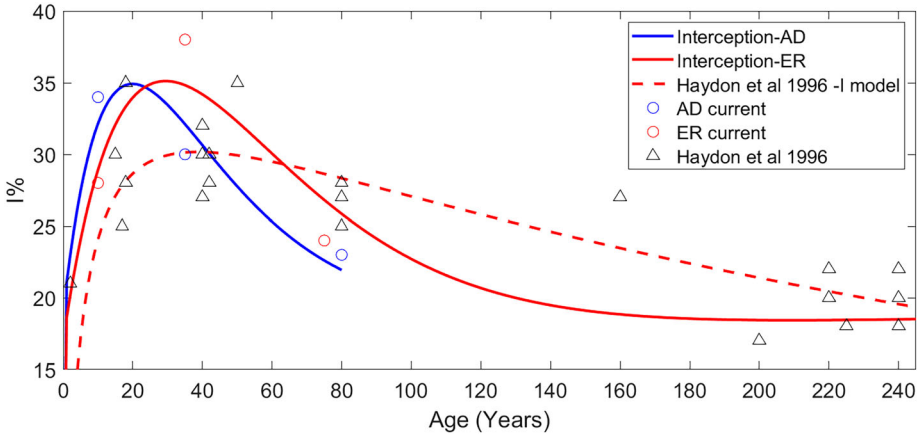



**FIGURE 8** Relationships between mean interception percentage and forest age showing plot-based estimates and fitted curves. Blue solid line is for *Acacia dealbata* forests. Solid red line and red dashed line represent canopy interception versus age fitted during the present study for *Eucalyptus regnans* forests and a study be Haydon et al. (1996) for *E. regnans* forests.

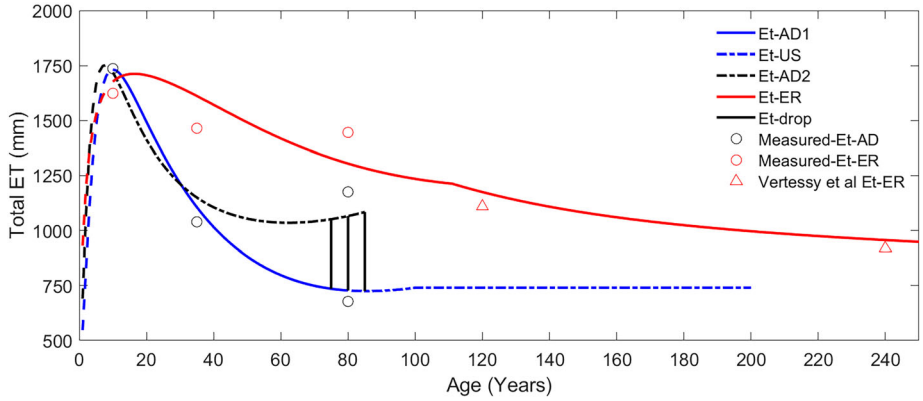



**FIGURE 9** The hypothesised total ET trajectories for *Acacia dealbata* and *Eucalyptus regnans* forests. The red solid line shows the average ET trajectory for *E. regnans* forests, blue solid line represents total annual ET with age if *Acacia* sapwood area declines gradually to near-zero at age 80, blue dashed line assumes no increase in annual ET after the death of *Acacia* overstorey. It is assumed that following the death of overstorey *A. dealbata* at age 80, the overstorey ET declines almost immediately to near-zero, while understorey ET is initially maintained at the same rate as just prior to overstorey death. The black dashed line and black vertical lines show annual total ET trajectories of *A. dealbata* forests if *Acacia* overstorey dies suddenly either at age 75, 80 or 85 years instead of a gradual decline in sapwood area.

age, the differences in overstorey transpiration between the two forests gradually increase, so that by age 35, overstorey transpiration varies widely between *E. regnans* and *A. dealbata* forests. This difference continues at least up until age 80.

## 3.5 | Long-term interception trajectories

The possible trends in long-term interception for the two forest types are shown in Figure 8. Dot points represent average interception rate of each age class for the two forests, estimated using throughfall and stem flow measurements in the water use plots.

## 3.6 | Long-term total ET trajectories of the two forest types

Two hypothetical trajectories were derived for total ET in *A. dealbata* forests (Figure 9). Given that at age 80 some *A. dealbata* stands were all dead, while others were still alive, it seems more likely that there is a sudden die-off of the overstorey at around age 80, which would result in a rapid reduction in overstorey interception and transpiration, in which case the shape of the ET trajectory in the late senescing stage may be more as depicted by the three vertical black lines in Figure 9: as soon as the overstorey dies, overstorey ET drops suddenly to near zero over a very short period of time. For example, during the monitoring of sap velocities in 80-year-old acacia Plot $TR_3$, one of the dominant overstorey *A. dealbata* trees died suddenly. Sap velocities in this tree began to decline about 3 weeks before visible crown death and were zero once the crown was completely dead.

The expected ET trajectories of *A. dealbata* forests confirm that the annual total ET of *A. dealbata* forests is less than that of *E. regnans* forests after age 10. Even the higher expected ET trajectory for *A. dealbata* in Figure 9 lies below the average ET line of *E. regnans* forests after age 10. This indicates that if *A. dealbata* forests replace *E. regnans* forests, long-term mean forest ET will be reduced. Overall, the results suggest that replacement of *E. regnans* forests with *A. dealbata* forests would result in a significant decrease in annual and decadal ET after about 20 years. Hence, the future direction of total ET in *A. dealbata* forests supports the acceptance of a hypothesis that

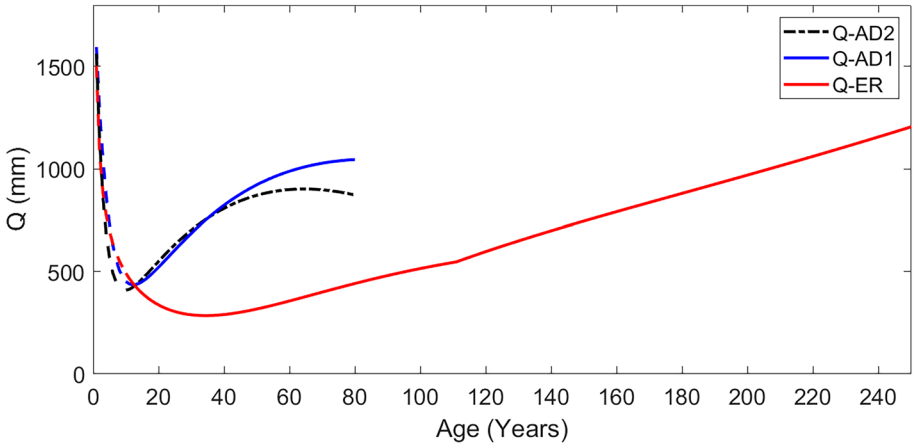



**FIGURE 10** Streamflow trajectories throughout their lifetime in *Eucalyptus regnans* and *Acacia dealbata* forests based on catchment-scale approximation of total ET curves for the two forest types, assuming mean annual rainfall is 1800 mm. Blue solid line represents water yield with age if *Acacia* sapwood area declines gradually to near-zero at age 80, the black dashed line shows water yield trajectory of *A. dealbata* forests if *Acacia* overstorey dies suddenly either at age 75, 80 or 85 years instead of a gradual decline in sapwood area, red solid line represents an approximation of catchment-scale water yield curve for *E. regnans* forests.

**TABLE 4** Plot-based estimates of annual water balance for *Acacia dealbata* and *Eucalyptus regnans* forests across the age sequence, assuming mean annual rainfall is 1800 mm.

| | 10 | | 35 | | 75/80 | |
|---|---|---|---|---|---|---|
| **Component** | ***A. dealbata*** | ***E. regnans*** | ***A. dealbata*** | ***E. regnans*** | ***A. dealbata*** | ***E. regnans*** |
| Transpiration (TOS) mm | 1030 | 1029 | 320 | 617 | 264 | 664 |
| Transpiration (TUS) mm | No understorey | No understorey | 25[a] | 50[a] | 145[a] | 233[a] |
| I_(OS) mm | 612 | 504 | 542 | 612 | 414 | 306 |
| I_(US) mm | No understorey | No understorey | 57 | 90 | 252 | 126 |
| Evp mm | 95 | 91 | 95 | 95 | 101 | 117 |
| ET (OS) mm | 1642 | 1533 | 862 | 1229 | 678 | 970 |
| ET (US) mm | 95 | 91 | 177 | 235 | 498 | 476 |
| ET (OS + US) mm | 1737 | 1624 | 1039 | 1464 | 1176 | 1446 |

*Note*: Overstorey transpiration (TOS), understorey transpiration (TUS), intercepted rainfall in mm by overstorey (I_OS), intercepted rainfall in mm by understorey (I_US), forest floor evaporation (Evp) and total ET in the two forests. ET of 75-year old *E. regnans* forests was estimated using data from Benyon et al. (2017).
[a]Estimated using data from Vertessy et al. (1998) and the present study (Table 2 and Sections 2.4 and 2.6).

the replacement of *E. regnans* forests with *A. dealbata* forests would result in a significant decrease in annual and decadal ET, inferring an increase in catchment water yield (Figure 10).

Table 4 shows the detailed estimation of annual water balance components of *E. regnans* and *A. dealbata* 10, 35 and 80-year-old stands. This field measured total ET (black circles in Figure 9) in *A. dealbata* forests closely matched with modelled total ET.

### 3.7 | Divergence in water yield between the two forest types

The catchment-scale approximation suggests that the maximum reduction of water yield in *A. dealbata* forests occurs at age 10 (Figure 10) compared to age 15–25 in *E. regnans* forests. The blue solid line depicts the water yield if the sapwood area of *A. dealbata* stands will gradually decline to zero by age 80. The black dashed line represents if *A. dealbata* overstorey is still alive at age 80. Either case suggests that water yield recovery in *A. dealbata* forests is faster than in *E. regnans* forests.

In contrast, the water yield increase in *E. regnans* forests after its hydrologically critical age (15–25 years) is more gradual and streamflow is expected to recover back to pre-fire levels much more slowly. Therefore, if *A. dealbata* replaces *E. regnans* forests, water yield in *A. dealbata* forests is expected to increase much more rapidly than in *E. regnans* forests.

## 4 | DISCUSSION

The present study provides a clear picture of divergence in ET and streamflow trajectories between *E. regnans* and *A. dealbata* forests

after climate/fire-driven species replacement in water supply catchments. These results are based on field measured observations over a considerable period. The measured forest hydrological parameters were combined using a stand scale dynamic modelling approach for understanding long-term implications for forest ET and water yield after this species replacement. ET dynamics related to the life cycle of *E. regnans* were in line with previous Australian studies (Benyon et al., 2015; Dunn & Connor, 1993; Vertessy et al., 1995, 2001). To our knowledge, this is the first study to measure ET dynamics in pure overstorey *A. dealbata* over a chronosequence and is the first to compare eco-hydrological functions between pure *E. regnans* and *A. dealbata* forests along an age sequence when both species occupy the same ecological niches. The outcome of this study provides insights on eco-hydrological implications of high-frequency fires for future water availability.

Our results indicate that the hydrological effects of multiple fires compared to single fires are different. Previous studies suggested that after a single disturbance, followed by recovery of the same vegetation type, hydrological equilibrium will eventually be restored, although this can take years to decades (Brookhouse et al., 2013; Feikema et al., 2013; Gharun et al., 2013; Lane et al., 2010; Nolan et al., 2014, 2015). However, the present study suggests that multiple disturbances, resulting in a change in the dominant vegetation, may cause a permanent change in ET and streamflow, with no return to pre-disturbance hydrological equilibrium. In this study, divergence in forest structure between *E. regnans* and *A. dealbata* forests was the primary driver of divergence in overstorey ET between the two forest types. No previous studies have investigated the effect of multiple burning and vegetation change on catchment water yield in south east Australia.

### 4.1 | Structural and functional divergence between *Eucalyptus regnans* and *Acacia dealbata* forests

Lakmali et al. (2022) discussed the structural changes in the overstorey of *E. regnans* and *A. dealbata* forests that resulted in divergence in overstorey transpiration between the two species. The addition of the other ET components, as presented here, confirms that divergence in total ET between *E. regnans* and *A. dealbata* forests with increasing forest age is also driven by increasing differences in forest structure between the two forests as they age. *E. regnans* and *A. dealbata* have similar regeneration and fire ecology and for at least the first 10 years after disturbance, structure of the two forest types is similar (Ashton, 1981). May (1999), after studying regeneration and growth dynamics of *E. regnans* in the presence of *A. dealbata*, suggested that growth of *A. dealbata* and *E. regnans* are similar for the first 30 years in their life cycles. However, Lakmali et al. (2022) and the present study, provide a clear indication that divergence in both forest structure and in eco-hydrologic functions such as overstorey transpiration, interception, total ET between the two forests is well underway by age 20.

Age-related structural divergence between *E. regnans* and *A. dealbata* forests may be partly related to differences in net primary productivity (NPP) between the forest types and how NPP is allocated. NPP is the difference between photosynthetic carbon production and autotropic respiration (Binkley et al., 1997). The allocation of NPP across biomass production and reproduction reveals important functional priorities of ecosystems (Malhi et al., 2011). *Acacia dealbata* forests put more effort into reproduction to ensure persistence over the long-term than *E. regnans*. The ecological literature confirms that regenerative abilities such as seed production in *A. dealbata* forests help to expand their occurrence in the landscape (Spalazzi et al., 2019). *Acacia dealbata* attains reproductive maturity after 4–5 years, compared to 15–25 years for *E. regnans* (Lindenmayer et al., 2011) and maintains a large seed bank in the soil which is continuously refilling by the release of a large number of seeds annually. *Acacia* seeds are protected by a hard seed coat, maintaining seed viability for a long time, enabling them to persist for a considerable period in the soil until conditions are favourable for germination, often just after fire (May, 1999). However, *E. regnans* seeds do not remain viable in the soil for long and therefore regeneration of *E. regnans* forest depends on seeds stored in the woody capsules in the crowns (Ashton, 1976). The regeneration potential of *A. dealbata* forests is, therefore, considerably higher than in *E. regnans*, suggesting that *A. dealbata* forests allocate a higher proportion of NPP to reproduction. These details confirm that the regeneration potential of *A. dealbata* forests is considerably superior than in *E. regnans* and therefore later *A. dealbata* forests will become the dominant vegetation type over the *E. regnans* forests. Further, in *A. dealbata* forests, the declining rate of increase of biomass after age 20 (Figure 6) is perhaps the result of this regeneration-oriented life cycle. The effect of regeneration potential may be more pronounced than the effect of the self-thinning process on forest structure in *A. dealbata* forests. As a result, compared to *E. regnans*, *A. dealbata* maintained a higher stocking density, but stem diameter and basal area growth reduced dramatically after age 20.

In contrast, tree height and diameter continue to increase in *E. regnans* well beyond age 80, so that by age 100, living aboveground biomass can be 350 Mg C $ha^{-1}$ (Volkova et al., 2018), indicating that *E. regnans* forests give functional priority to biomass production but at the expense of reproduction potential. The differences in NPP allocation and changes in reproduction potential together may explain the divergence in stand structure between *E. regnans* and *A. dealbata* forests.

### 4.2 | Changes in eco-hydrological functions and total ET between the two forest types over a chronosequence

Changes in structural properties and functional processes that occur through forest development stages in different forest types influence eco-hydrological processes (Bond et al., 2007; Jones & Post, 2004). This study shows that differences in eco-hydrologic processes

between *E. regnans* and *A. dealbata* forests were driven by differences in stand structure that increased with forest age, resulting in divergence in ET between the two forest types across the age sequence. Annual ET values were higher in *A. dealbata* during the first 10 years of their lifetime in comparison to *E. regnans*, due primarily to higher initial stocking density in *A. dealbata*. More rapid reduction in annual ET in *A. dealbata* between age 20 and age 80 was due primarily to more rapid declines in overstorey transpiration and canopy interception. These findings are in line with previous studies on ET partitioning between different forest stands (Ford et al., 2010; Vertessy et al., 1998). In *E. regnans* and *A. dealbata* forests, mean annual transpiration is largely explained by forest sapwood area, which is controlled by stand density and mean proportional sapwood thickness (Lakmali et al., 2022). Rapid slowing of basal area and dbh increment in *A. dealbata* after age 20 results in a rapid reduction in sapwood area (Figure 6) and therefore in transpiration as stand density reduces (Lakmali et al., 2022).

That forest structure controls ET in *E. regnans* is in agreement with the findings of Haydon et al. (1996) and Vertessy et al. (2001), but significantly extends our understanding of the age-ET dynamics since we incorporated understorey ET into the ET trajectories. Thus, this study has refined our understanding of the *E. regnans* age-ET response. In *A. dealbata* forests, we found strong connections between age-related changes in forest structure, overstorey transpiration and total ET, which is consistent with *E. regnans*. Further, the present study provides new knowledge on ET in *A. dealbata* forests which shows that while the trend in ET with age is broadly similar to *E. regnans*, it occurs much more rapidly, with the rate of ET recovery to pre-disturbance level being much faster in *A. dealbata* than in *E. regnans*.

Increasing understorey density can off-set the reduction in overstorey transpiration in old-growth forests (Delzon & Loustau, 2005; Vertessy et al., 2001). In our study, overstorey LAI decreased from 2.7 in 35-year-old *Acacia* to 2.2 in 80-year-old *Acacia*, while understorey LAI increased from 0.2 to 1.15. In senescing *A. dealbata* forests, the understorey transpiration contribution (29.8%) to system ET was similar to that of overstorey transpiration (31.2%), indicating the understorey and overstorey contribute equally to total ET at the final stage of *Acacia* forests. In *E. regnans* at age 75, understorey contribution to total ET (16%) was not as high as in *A. dealbata* at age 80 because understorey was not as developed in *E. regnans* forests as much as in similar-aged *Acacia* forests. Based on measurements in the water use plots, understorey ET was considerably higher in senescing *Acacia* stands compared to *E. regnans* forests of similar age. The development of denser understorey vegetation in old-growth *Acacia* forests is due to canopy openness in the overstorey at the senescing stage, permitting higher solar radiation to the lower strata of the forest. Observations of large areas of dead *A. dealbata* overstorey in many other stands regenerated in 1939 suggests that at around 80 years of age there is a sudden death of the *Acacia* overstorey in their late senescing stage. The immediate effect of this would be the loss of all overstorey transpiration and most of the overstorey interception. The effect of this on understorey ET is uncertain. Whether ET from understorey eventually increases to partly or fully off-set the reduction in overstorey ET, and how long this will take, is unknown. Accordingly, the holistic view of this ET study suggests that if *A. dealbata* replaces *E. regnans*, the ET regime will initially shift to one dominated by *Acacia* but by the end of the ~80 year *Acacia* life cycle, the ET regime is beginning to transition into another new state dominated by shrubby understorey species. Major sources of uncertainties in the ET trajectory of *Acacia* forests are mortality rates in old-growth *Acacia* forests and ET dynamics in the post-*Acacia* phase. In the absence of further fires, the next ET regime after the *A. dealbata* phase will be dominated by forests of shrubby understorey species and ferns. The magnitude of ET in the post-*Acacia* phase is uncertain due to uncertainty in the species mix of the understorey. Thus, comprehensive knowledge of shrubby vegetation (ET rates, composition and structure) is essential to complete the story of ecological tipping points, alternative stable states and transition of ET regimes across different vegetation phases in obligate seeder *E. regnans* forests.

### 4.3 | Water yield implications

Water yield predicted for *E. regnans* forests during the present study (Figure 10), which was based on functional relationships of long-term forest eco-hydrological processes (using plot-scale data), is qualitatively consistent with the water yield and forest age relationship of Kuczera (1987). Long-term ET trajectories derived in the present study showed maximum water use at ~10 years of age in *A. dealbata* forests while for *E. regnans* forests, it was at around age 20–25. The Kuczera curve similarly indicates that water yield is significantly lower in regrowth *E. regnans* forests than in old-growth forests. This indication of water yield difference between old-growth and regrowth *E. regnans* is due to differences in ET between old-growth and regrowth (Haydon et al., 1996; Vertessy et al., 2001). High post-fire seedling densities in the two forests types drive the initial peak in ET. Subsequent age-related ET reductions are attributable to age-related reductions in stand density, sapwood area, and LAI. The predicted streamflow trend with age in *E. regnans* in this study is qualitatively comparable with Haydon et al. (1996). Although understorey ET was not considered by Haydon et al. (1996) when determining water yield from *E. regnans*, the present study accounts for both overstorey and understorey ET in *E. regnans* forests.

The trends in ET dynamics highlight that changing the catchment vegetation from *E. regnans* to *A. dealbata* forests would alter streamflow in the long-term. Precise prediction of water yield amounts is beyond the scope of this research, but based on likely long-term ET trajectories (Figure 9), replacement of *E. regnans* forests with *A. dealbata* would decrease annual and decadal ET after about 10 years, inferring an increase in catchment water yield (Figure 10). There is a significant possibly that further fire events would occur in the acacia stands, thereby 'resetting the clock' and resulting in higher ET for the first 10–15 years. How repeated short-interval fires may effect acacia regeneration is not known, but there are examples of acacia stands transitioning into what is describes as 'scrub'—a mix of

understorey species with no clear dominant species. It is likely scrub would have similar water use to the acacias, but there are no observations to confirm this.

### 4.4 | Multiple burns, tipping points, eco-hydrologic thresholds, ET regimes shift and non-equilibrium concept

The significant divergences in forest structure, ET and water yield between *E. regnans* and *A. dealbata* forests after age 20 imply that resultant eco-hydrological changes fit more with the ideas of non-equilibrium. Here, we found that if *A. dealbata* replaces *E. regnans* forests, ET rates will be significantly decreased, so that the alternative vegetation phase will not move closer to the previous dominant state (will not maintain similar rates of ET) which is a contrast to the equilibrium concept. The equilibrium concept and equilibrium theories are useful for explaining temporal dynamics of stable ecological systems. Classical equilibrium concepts (balance of nature) are inadequate to explain the temporal dynamics of unstable communities (Mori, 2011). This is leading to paradigm shifts in ecological concepts from equilibrium to non-equilibrium theories for understanding instability and abrupt changes in ecosystems occurring beyond the natural balance. The non-equilibrium theory is based on unstable conditions and can address changes in vegetation that are linked to climate change (Sprugel, 1991). A shift in vegetation and related changes in ET observed in the present study does not comply with Eagleson's optimality theory (Eagleson & Tellers, 1982), as the observed changes are more in line with non-equilibrium theories.

In many fire-prone forests across the globe, fire return intervals are reducing from a century or more to decades or less (Turner et al., 2019). As a result, climate-fire-vegetation links are changing (Johnstone et al., 2016). Following frequent disturbances, some ecosystems can recover to their original state, but other ecosystems shift towards a new state (Fletcher et al., 2013). Under such climate-induced fire regime changes, obligate seeder forests around the world are becoming highly vulnerable to alterations in their successional trajectories (Brown & Johnstone, 2012; Enright et al., 2015; Johnstone et al., 2010; Keeley et al., 1999; Savage & Mast, 2005). Our results imply that after high-frequency fires, once *A. dealbata* replaces *E. regnans*, pyro-eco-hydrologic thresholds are altered, leading to a new hydrologic state. When forests experience such compound disturbances, they fail to achieve ecological resilience (Kleinman et al., 2019). With increased occurrence of high-frequency wildfires, *A. dealbata* also may not reach its 80 years of life span. The existence of mature stands of both species considered in this study is largely a function of the historical climate (i.e., cool and wet). The majority of *A. dealbata* stands in the central highlands of Victoria have recently completed the full life cycle and are now close to 100% mortality at age 80. Their origin was the 1926 and 1939 fires. The next successional phase is 'scrub'—a mix of understorey shrubs and small trees. This also occurs where increasing fire frequency has led to create patches with multiple burning.

However, there are also areas where both *E. regnans* and their replacement species, *A. dealbata*, have both been early extirpation of both *E. regnans* and *A. dealbata* (and other acacia species) from their native habitats. Brown et al. (2021) investigated how forest structure influences fuel moisture in alternative forest states in southeast Australia. They suggested that Acacia forests would transition into the non-eucalyptus forest over time. However, this alternative forest type is likely unstable, depicting a negative fire-vegetation-climate feedback loop. Under these circumstances, forests cannot attain an equilibrium state (Holling, 1973) and therefore, pass an ecological tipping point. This study suggests that the *E. regnans* forests of southeast Australia is one such ecosystem.

### 4.5 | Uncertainties associated with the present study

This study provides insights for understanding catchment-scale divergence in ET and streamflow between the two forest types. However, there are several sources of uncertainty in the study that must be noted.

The first is regarding the sap flow and microclimate data. Difficulties encountered with the experimental set up, relevant data processing and cross validations were explained in the Lakmali et al. (2022).

Second, this study used the measured data during the study period plus previously measured data and published data in the literature. Integrating data from different sources may create some uncertainty. All data sets were checked for compatibility in terms of climate, locality and the same measurement period of the year before using them in the ET analysis. However, there are bound to be noise in these data, but we are confident that we have not used these data out of context and acknowledge the issue.

Third, root zone soil moisture was estimated using the AWRA-Lv6 model (The Australian Landscape Water Balance Model [Frost et al., 2018]) and used to identify water-limited sap velocity responses in this study to compensate for the lack of direct measurements on root zone soil moisture. We acknowledge this is a modelled product, but it is well tested and widely used in Australia. We contend that errors in these data would not have a significant impact on our overall results.

Fourthly, modelling ET and streamflow through time assumes trajectories of vegetation dynamics are spatially homogenous. The dynamic ET models could be upgraded to catchment-scale for improved quantitative assessments of future water availability by accounting for catchment-scale spatial heterogeneity in the sapwood area modelling, since forest ET is strongly controlled by this stand structural variable. The present study was constrained by time and resources, preventing the extension of the results up to that level. Future research will need to account for the spatial heterogeneity in large catchments. A Lidar-based technique is considered the best option for quantifying spatial heterogeneity in stand structure and linking this to streamflow (Jaskierniak et al., 2016, 2019).

Finally, in the absence of further fires, the next ET regime after the *A. dealbata* phase will be dominated by forests of shrubby understorey species and ferns. The magnitude of ET in the post-*Acacia* phase is uncertain due to uncertainty in the species mix of the understorey. Thus, evapotranspiration dynamics in the post-*Acacia* phase is another dimension of future research, although it seems unlikely that water use of this vegetation would exceed that of the *A. dealbata* stands.

## 5 | CONCLUSION

The findings of this study support a hypothesis that replacement of *E. regnans* with *A. dealbata* forests would result in a significant decrease in annual and decadal ET, inferring an increase in catchment water yield. The data suggest that significant divergence in forest structure, ET and water yield between *E. regnans* and *A. dealbata* forests has started by age 20 years, implying that replacement of *E. regnans* with *A. dealbata* under high-frequency fire conditions results in a non-equilibrium state. Understorey contribution to the system water balance was significantly higher in *A. dealbata* forests in their senescing stage. This suggests that, after the *Acacia* life cycle finishes, the ET regime will transit into a new state that will be dominated by shrubby understorey species. Accordingly, if *A. dealbata* replaces *E. regnans*, the ET regime will initially shift to one dominated by *Acacia* but by the end of the ~80 year *Acacia* life cycle, the ET regime is beginning to transition into another new hydrologic state dominated by shrubby understorey species. Overall, this study shows that fire frequency thresholds can trigger eco-hydrologic divergence in fire-prone forest systems.

### ACKNOWLEDGEMENTS

This research was funded by the Integrated Forest Ecosystem Research project, Victorian Department of Environment, Land, Water and Planning, and by Melbourne Water. Melbourne University International Research Scholarship and a top-up scholarship (IFER Project) provided financial assistance throughout this research period. Further, a Postgraduate Writing-up Award granted by the Albert Shimmins Fund (University of Melbourne) is acknowledged for the financial assistance during the writing-up period of this manuscript.

### CONFLICT OF INTEREST STATEMENT

Authors confirmed no conflict of interest.

### DATA AVAILABILITY STATEMENT

The data that support the findings of this study are available from the corresponding author upon reasonable request.

### ORCID

*Shyanika Lakmali* https://orcid.org/0000-0002-5686-1825

### REFERENCES

Ashton, D. H. (1976). The development of even-aged stands of *Eucalyptus regnans* F. Muell. in Central Victoria. *Australian Journal of Botany*, *24*(3), 397–414. https://doi.org/10.1071/BT9760397

Ashton, D. H. (1981). Fire in tall open forests (wet sclerophyll forests). In A. M. Gill, R. H. Groves, & I. R. Noble (Eds.), *Fire and Australian biota* (pp. 339–366). Australian Academy of Science.

Benyon, R. G., Lane, P. N. J., Jaskierniak, D., Kuczera, G., & Haydon, S. R. (2015). Use of a forest sapwood area index to explain long-term variability in mean annual evapotranspiration and streamflow in moist eucalypt forests. *Water Resources Research*, *51*(7), 5318–5331. https://doi.org/10.1002/2015wr017321

Benyon, R. G., Nolan, R. H., Hawthorn, S. N. D., & Lane, P. N. J. (2017). Stand-level variation in evapotranspiration in non-water-limited eucalypt forests. *Journal of Hydrology*, *551*, 233–244. https://doi.org/10.1016/j.jhydrol.2017.06.002

Binkley, D., O'Connell, A. M., & Sankaran, K. V. (1997). Stand development and productivity. In E. K. S. Nambiar, A. Sandanandan, & G. Brown (Eds.), *Management of soil, nutrients and water in tropical plantation forests* (pp. 419–442). Australian Centre for International Agricultural Research.

Bond, B. J., Meinzer, F. C., & Brooks, J. R. (2007). How trees influence hydrological cycles in forest ecosystems. In P. J. Wood, D. M. Hannah, & J. P. Sadler (Eds.), *Hydroecology and ecohydrology; past, present and future* (pp. 7–52). John Wiley and Sons Ltd.

Bowman, D. M. J. S., Murphy, B. P., Neyland, D. L. J., Williamson, G. J., & Prior, L. D. (2014). Abrupt fire regime change may cause landscape-wide loss of mature obligate seeder forests. *Global Change Biology*, *20*(3), 1008–1015. https://doi.org/10.1111/gcb.12433

Bowman, D. M. J. S., Williamson, G. J., Prior, L. D., & Murphy, B. P. (2016). The relative importance of intrinsic and extrinsic factors in the decline of obligate seeder forests. *Global Ecology and Biogeography*, *25*(10), 1166–1172. https://doi.org/10.1111/geb.12484

Bren, L., & Hopmans, P. (2007). Paired catchments observations on the water yield of mature eucalypt and immature radiata pine plantations in Victoria, Australia. *Journal of Hydrology*, *336*(3–4), 416–429. https://doi.org/10.1016/j.jhydrol.2007.01.018

Bren, L., Lane, P., & Hepworth, G. (2010). Longer-term water use of native eucalyptus forest after logging and regeneration: The Coranderrk experiment. *Journal of Hydrology*, *384*(1–2), 52–64. https://doi.org/10.1016/j.jhydrol.2010.01.007

Brookhouse, M. T., Farquhar, G. D., & Roderick, M. L. (2013). The impact of bushfires on water yield from south East Australia's ash forests. *Water Resources Research*, *49*(7), 4493–4505. https://doi.org/10.1002/wrcr.20351

Brown, C. D., & Johnstone, J. F. (2012). Once burned, twice shy: Repeat fires reduce seed availability and alter substrate constraints on *Picea mariana* regeneration. *Forest Ecology and Management*, *266*, 34–41. https://doi.org/10.1016/j.foreco.2011.11.006

Brown, T. P., Inbar, A., Duff, T. J., Burton, J., Noske, P. J., Lane, P. N., & Sheridan, G. (2021). Forest structure drives fuel moisture response across alternative forest states. *Fire*, *4*(3), 48. https://doi.org/10.3390/fire4030048

Buma, B., Brown, C. D., Donato, D. C., Fontaine, J. B., & Johnstone, J. F. (2013). The impacts of changing disturbance regimes on serotinous plant populations and communities. *Bioscience*, *63*(11), 866–876. https://doi.org/10.1525/bio.2013.63.11.5

Burgess, S. S. O., Adams, M. A., Turner, N. C., Beverly, C. R., Ong, C. K., Ahmed, A. H. K., & Bleby, T. M. (2001). An improved heat pulse method to measure low and reverse rates of sap flow in woody plants. *Tree Physiology*, *21*, 589–598. https://doi.org/10.1093/treephys/21.9.589

Burns, E. L., Lindenmayer, D. B., Stein, J., Blanchard, W., McBurney, L., Blair, D., & Banks, S. C. (2015). Ecosystem assessment of mountain ash forest in the central highlands of Victoria, South-Eastern Australia. *Austral Ecology*, *40*(4), 386–399. https://doi.org/10.1111/aec.12200

De Jong, S. M., & Jetten, V. G. (2007). Estimating spatial patterns of rainfall interception from remotely sensed vegetation indices and spectral mixture analysis. *International Journal of Geographical Information Science*, *21*(5), 529–545. https://doi.org/10.1080/13658810601064884

Delzon, S., & Loustau, D. (2005). Age-related decline in stand water use: Sap flow and transpiration in a pine forest chronosequence. *Agricultural and Forest Meteorology*, *129*(3–4), 105–119. https://doi.org/10.1016/j.agrformet.2005.01.002

Dunn, G. M., & Connor, D. J. (1993). An analysis of sap flow in mountain ash (*Eucalyptus regnans*) forests of different age. *Tree Physiology*, *13*(4), 321–336. https://doi.org/10.1093/treephys/13.4.321

Eagleson, P. S., & Tellers, T. E. (1982). Ecological optimality in water-limited natural soil-vegetation systems: 2. Tests and applications. *Water Resources Research*, *18*(2), 341–354. https://doi.org/10.1029/WR018i002p00341

Enright, N. J., Fontaine, J. B., Bowman, D. M. J. S., Bradstock, R. A., & Williams, R. J. (2015). Interval squeeze: Altered fire regimes and demographic responses interact to threaten woody species persistence as climate changes. *Frontiers in Ecology and the Environment*, *13*(5), 265–272. https://doi.org/10.1890/140231

Fagg, P., Lutze, M., Slijkerman, C., Ryan, M., & Bassett, O. (2013). Silvicultural recovery in ash forests following three recent large bushfires in Victoria. *Australian Forestry*, *76*(3–4), 140–155. https://doi.org/10.1080/00049158.2013.848610

Fairman, T. A., Nitschke, C. R., & Bennett, L. T. (2016). Too much, too soon? A review of the impacts of increasing wildfire frequency on tree demography and structure in temperate forests. *International Journal of Wildland Fire*, *25*(8), 831–848. https://doi.org/10.1071/WF15010

Feikema, P. M., Sherwin, C. B., & Lane, P. N. J. (2013). Simulating the combined effects of climate and wildfire on streamflow. In *Proceedings – 20th international congress on modelling and simulation* (pp. 2848–2854). MODSIM. https://doi.org/10.36334/modsim.2013.l13.feikema

Fletcher, M. S., Wood, S. W., & Haberle, S. G. (2013). A fire driven shift from forest to non-forest: Evidence for alternative stable states? *Ecology*, *95*(9), 2504–2513. https://doi.org/10.1890/12-1766.1

Ford, C. R., Hubbard, R. M., & Vose, J. M. (2010). Quantifying structural and physiological controls on variation in canopy transpiration among planted pine and hardwood species in the Southern Appalachians. *Ecohydrology*, *4*, 183–195. https://doi.org/10.1002/eco.136

Frost, A. J., Ramchurn, A., & Smith, A. (2018). *The Australian Landscape Water Balance model (AWRA-L v6). Technical description of the Australian Water Resources Assessment Landscape model version 6*, Technical report. Bureau of Meteorology.

Gharun, M., Turnbull, T. L., & Adams, M. A. (2013). Stand water use status in relation to fire in a mixed species eucalypt forest. *Forest Ecology and Management*, *304*, 162–170. https://doi.org/10.1016/j.foreco.2013.05.002

Ghimire, C. P., Bruijnzeel, L. A., Lubczynski, M. W., Ravelona, M., Zwartendijk, B. W., & van Meerveld, H. J. I. (2017). Measurement and modelling of rainfall interception by two differently aged secondary forests in upland eastern Madagascar. *Journal of Hydrology*, *545*, 212–225. https://doi.org/10.1016/j.jhydrol.2016.10.032

Gou, J., Miao, C., Samaniego, L., Xiao, M., Wu, J., & Guo, X. (2021). A high-quality natural runoff dataset for hydrological and climate studies in China. *Bulletin of the American Meteorological Society*, *102*, E929–E947. https://doi.org/10.1175/bams-d-20-0094.1

Halofsky, J. E., Peterson, D. L., & Harvey, B. H. (2020). Changing wildfire, changing forests: The effects of climate change on fire regimes and vegetation in the Pacific Northwest, USA. *Fire Ecology*, *16*(1), 2–26. https://doi.org/10.1186/s42408-019-0062-8

Hawthorne, S. N. D., Benyon, R. G., & Lane, P. N. J. (2018). Changes in evapotranspiration components following replacement of *Eucalyptus regnans* with *Acacia* species. *Hydrological Processes*, *32*(2), 241–252. https://doi.org/10.1002/hyp.11410

Hawthorne, S. N. D., Lane, P. N. J., Bren, L. J., & Sims, N. C. (2013). The long-term effects of thinning treatments on vegetation structure and water yield. *Forest Ecology and Management*, *310*, 983–993. https://doi.org/10.1016/j.foreco.2013.09.046

Haydon, S. R., Benyon, R. G., & Lewis, R. (1996). Variation in sapwood area and throughfall with forest age in mountain ash (*Eucalyptus regnans* F. Muell.). *Journal of Hydrology*, *187*(3–4), 351–366. https://doi.org/10.1016/S0022-1694(96)03016-8

Holling, C. S. (1973). Resilience and stability of ecological systems. *Annual Review of Ecology and Systematics*, *4*(1), 1–23. https://doi.org/10.1146/annurev.es.04.110173.000245

Huf, B., & Mclean, H. (2020). *2019–20 Bushfires, research note, No. 1*. Parliamentary Library and Information Service, Parliament of Victoria.

Jaskierniak, D., Kuczera, G., Benyon, R. G., Haydon, S., & Lane, P. N. J. (2019). Top-down seasonal streamflow model with spatiotemporal forest sapwood area. *Journal of Hydrology*, *568*, 372–384. https://doi.org/10.1016/j.jhydrol.2018.10.075

Jaskierniak, D., Kuczera, G., Benyon, R. G., & Lucieer, A. (2016). Estimating tree and stand sapwood area in spatially heterogeneous southeastern Australian forests. *Journal of Plant Ecology*, *9*(3), 272–284. https://doi.org/10.1093/jpe/rtv056

Johnstone, J. F., Allen, C. D., Franklin, J. F., Frelich, L. E., Harvey, B. J., Higuera, P. E., Mack, M. C., Meentemeyer, R. K., Metz, M. R., Perry, G. L. W., Schoennagel, T., & Turner, M. G. (2016). Changing disturbance regimes, ecological memory, and forest resilience. *Frontiers in Ecology and the Environment*, *14*(7), 369–378. https://doi.org/10.1002/fee.1311

Johnstone, J. F., Chapin, F. S., Hollingsworth, T. N., Mack, M. C., Romanovsky, V., & Turetsky, M. (2010). Fire, climate change, and forest resilience in interior Alaska. *Canadian Journal of Forest Research*, *40*(7), 1302–1312. https://doi.org/10.1139/X10-061

Jones, J. A., & Post, D. A. (2004). Seasonal and successional streamflow response to forest cutting and regrowth in the northwest and eastern United States. *Water Resources Research*, *40*(5), 1–19. https://doi.org/10.1029/2003WR002952

Keeley, J. E., Ne'eman, G., & Fotheringham, C. J. (1999). Immaturity risk in a fire dependent pine. *Journal of Mediterranean Ecology*, *1*, 41–48.

Khaledi, J., Nitschke, C., Lane, P. N. J., Penman, T., & Nyman, P. (2022). The influence of atmosphere-ocean phenomenon on water availability across temperate Australia. *Water Resources Research*, *58*(1), e2020WR029409. https://doi.org/10.1029/2020wr029409

Kleinman, J. S., Goode, J. D., Fries, A. C., & Hart, J. L. (2019). Ecological consequences of compound disturbances in forest ecosystems: A systematic review. *Ecosphere*, *10*(11), e02962. https://doi.org/10.1002/ecs2.2962

Kuczera, G. (1987). Prediction of water yield reductions following a bushfire in ash-mixed species eucalypt forest. *Journal of Hydrology*, *94*(3–4), 215–236. https://doi.org/10.1016/0022-1694(87)90054-0

Lakmali, S., Benyon, R. G., Sheridan, G. J., & Lane, P. N. J. (2022). Change in fire frequency drives a shift in species composition in native *Eucalyptus regnans* forests; implications for overstorey forest structure and transpiration. *Ecohydrology*, *15*(3), e2412. https://doi.org/10.1002/eco.2412

Lane, P. N. J., Feikema, P. M., Sherwin, C. B., Peel, M. C., & Freebairn, A. C. (2010). Modelling the long-term water yield impact of wildfire and other forest disturbance in eucalypt forests. *Environmental Modelling and Software*, *25*(4), 467–478. https://doi.org/10.1016/j.envsoft.2009.11.001

Lane, P. N. J., & Mackay, S. M. (2001). Stream flow response of mixed-species eucalypt forests to patch cutting and thinning treatments. *Forest Ecology and Management*, *143*, 131–142. https://doi.org/10.1016/S0378-1127(00)00512-0

Langford, K. J. (1976). Change in yield of water following a bushfire in a forest of *Eucalyptus regnans*. *Journal of Hydrology*, *29*(1–2), 87–114. https://doi.org/10.1016/0022-1694(76)90007-X

Lindenmayer, D. (2016). The importance of managing and conserving large old trees: A case study from victorian mountain ash forests. *Proceedings of the Royal Society of Victoria*, *128*(1), 64–70. https://doi.org/10.1071/RS16006

Lindenmayer, D. B., Hobbs, R. J., Likens, G. E., Krebs, C. J., & Banks, S. C. (2011). Newly discovered landscape traps produce regime shifts in wet forests. *Proceedings of the National Academy of Sciences of the United States of America*, *108*(38), 15887–15891. https://doi.org/10.1073/pnas.1110245108

Macfarlane, C., Arndt, S. K., Livesley, S. J., Edgar, A. C., White, D. A., Adams, M. A., & Eamus, D. (2007). Estimation of leaf area index in eucalypt forest with vertical foliage, using cover and full-frame fisheye photography. *Forest Ecology and Management*, *242*(2–3), 756–763. https://doi.org/10.1016/j.foreco.2007.02.021

Malhi, Y., Doughty, C., & Galbraith, D. (2011). The allocation of ecosystem net primary productivity in tropical forests. *Philosophical Transactions of the Royal Society B: Biological Sciences*, *366*(1582), 3225–3245. https://doi.org/10.1098/rstb.2011.0062

Marshall, D. C. (1958). Measurements of sap flow in conifers. *Plant Physiology*, *33*(6), 385–396. https://doi.org/10.1104/pp.33.6.385

May, B. (1999). *Silver wattle (Acacia dealbata): Its role in the ecology of the mountain ash forest and the effect of alternative silvicultural systems on its regeneration* (PhD thesis). Department of Botany, The University of Melbourne.

McColl-Gausden, S. C., Bennett, L. T., Clarke, H., Ababei, D., & Penman, T. D. (2022). The fuel–climate–fire conundrum: How will fire regimes change in temperate eucalypt forests under climate change? *Global Change Biology*, *28*(17), 5211–5226. https://doi.org/10.1111/gcb.16283

Mirus, B. B., Ebel, B. A., Mohr, C. H., & Zegre, N. (2017). Disturbance hydrology: Preparing for an increasingly disturbed future. *Water Resources Research*, *53*(12), 10007–10016. https://doi.org/10.1002/2017wr021084

Mitchell, P. J., Benyon, R. G., & Lane, P. N. J. (2012). Responses of evapotranspiration at different topographic positions and catchment water balance following a pronounced drought in a mixed species eucalypt forest, Australia. *Journal of Hydrology*, *440–441*, 62–74. https://doi.org/10.1016/j.jhydrol.2012.03.026

Mori, A. S. (2011). Ecosystem management based on natural disturbances: Hierarchical context and non-equilibrium paradigm. *Journal of Applied Ecology*, *48*(2), 280–292. https://doi.org/10.1111/j.1365-2664.2010.01956.x

Murphy, B. P., Bradstock, R. A., Boer, M. M., Carter, J., Cary, G. J., Cochrane, M. A., Fensham, R. J., Russell-Smith, J., Williamson, G. J., & Bowman, D. M. J. S. (2013). Fire regimes of Australia: A pyrogeographic model system. *Journal of Biogeography*, *40*(6), 1048–1058. https://doi.org/10.1111/jbi.12065

Niemeyer, R. J., Bladon, K. D., & Woodsmith, R. D. (2020). Long-term hydrologic recovery after wildfire and post-fire forest management in the interior Pacific Northwest. *Hydrological Processes*, *34*, 1182–1197. https://doi.org/10.1002/hyp.13665

Nolan, R. H., Lane, P. N. J., Benyon, R. G., Bradstock, R. A., & Mitchell, P. J. (2014). Changes in evapotranspiration following wildfire in resprouting eucalypt forests. *Ecohydrology*, *7*, 1363–1377. https://doi.org/10.1002/eco.1463

Nolan, R. H., Lane, P. N. J., Benyon, R. G., Bradstock, R. A., & Mitchell, P. J. (2015). Trends in evapotranspiration and streamflow following wildfire in resprouting eucalypt forests. *Journal of Hydrology*, *524*, 614–624. https://doi.org/10.1016/j.jhydrol.2015.02.045

Ruprecht, J. K., & Schofield, N. J. (1991). Effects of partial deforestation on hydrology and salinity in high salt storage landscapes. I. Extensive block clearing. *Journal of Hydrology*, *129*(1–4), 19–38. https://doi.org/10.1016/0022-1694(91)90042-g

Savage, M., & Mast, J. N. (2005). How resilient are southwestern ponderosa pine forests after crown fires? *Canadian Journal of Forest Research*, *35*(4), 967–977. https://doi.org/10.1139/x05-028

Spalazzi, F., Tecco, P. A., & Funes, G. (2019). Overcoming lag phase: Do regenerative attributes onset *Acacia dealbata* spread in a newly invaded system? *Australian Journal of Botany*, *67*(1), 46–54. https://doi.org/10.1071/BT18097

Sprugel, D. G. (1991). Disturbance, equilibrium, and environmental variability: What is "natural" vegetation in a changing environment? *Biological Conservation*, *58*(1), 1–18. https://doi.org/10.1016/0006-3207(91)90041-7

Turner, M. G., Braziunas, K. H., Hansen, W. D., & Harvey, B. J. (2019). Short-interval severe fire erodes the resilience of subalpine lodgepole pine forests. *Proceedings of the National Academy of Sciences of the United States of America*, *166*(23), 11319–11328. https://doi.org/10.1073/pnas.1902841116

Van Dijk, A. I. J. M., & Bruijnzeel, L. A. (2001). Modelling rainfall interception by vegetation of variable density using an adapted analytical model. Part 1. Model description. *Journal of Hydrology*, *247*, 230–238. https://doi.org/10.1016/S0022-1694(01)00392-4

Vertessy, R. A., Benyon, R. G., O'Sullivan, S. K., & Gribben, P. R. (1995). Relationships between stem diameter, sapwood area, leaf area and transpiration in a young mountain ash forest. *Tree Physiology*, *15*(9), 559–567. https://doi.org/10.1093/treephys/15.9.559

Vertessy, R. A., Watson, F. G. R., & O'Sullivan, S. K. (2001). Factors determining relations between stand age and catchment water balance in mountain ash forests. *Forest Ecology and Management*, *143*(1–3), 13–26. https://doi.org/10.1016/S0378-1127(00)00501-6

Vertessy, R. A., Watson, F. G. R., O'Sullivan, S. K., Davis, S. H., Campbell, R., Benyon, R. J., & Haydon, S. R. (1998). *Predicting water yield from mountain ash forest catchments*. Industry Report No. 98/4. Cooperative Research Centre for Catchment Hydrology.

Volkova, L., Roxburgh, S. H., Weston, C. J., Benyon, R. G., Sullivan, A. L., & Polglase, P. J. (2018). Importance of disturbance history on net primary productivity in the world's most productive forests and implications for the global carbon cycle. *Global Change Biology*, *24*(9), 4293–4303. https://doi.org/10.1111/gcb.14309

Ward, P. R., & Micin, S. F. (2006). The capacity of dryland lucerne for groundwater uptake. *Australian Journal of Agricultural Research*, *57*(5), 483–487. https://doi.org/10.1071/AR05311

Watson, F., Vertessy, R., McMahon, T., Rhodes, B., & Watson, I. (2001). Improved methods to assess water yield changes from paired-catchment studies: Application to the Maroondah catchments. *Forest Ecology and Management*, *143*(1–3), 189–204. https://doi.org/10.1016/S0378-1127(00)00517-X

Watson, F. G. R. (1998). *Large scale, long-term, physically based modelling of the effects of the land cover change on forest water yield* (PhD thesis). Department of Civil and Environmental Engineering. Doctor of Philosophy, The University of Melbourne, Australia.

Webb, A. A., Kathuria, A., & Turner, L. (2012). Longer-term changes in streamflow following logging and mixed species eucalypt forest regeneration: The Karuah experiment. *Journal of Hydrology*, *464–465*, 412–422. https://doi.org/10.1016/j.jhydrol.2012.07.034

Welles, J. M., & Norman, J. M. (1991). Instrument for indirect measurement of canopy architecture. *Agronomy Journal*, *83*(5), 818–825. https://doi.org/10.2134/agronj1991.00021962008300050009x

White, P. S., & Jentsch, A. (2001). The search for generality in studies of disturbance and ecosystem dynamics. In K. Esser, U. Luttge, J. W. Kadereit, & W. Beyschlag (Eds.), *Progress in Botany* (Vol. 62). Springer, Berlin, Heidelberg. https://doi.org/10.1007/978-3-642-56849-7_17

## SUPPORTING INFORMATION

Additional supporting information can be found online in the Supporting Information section at the end of this article.

**How to cite this article:** Lakmali, S., Benyon, R. G., Sheridan, G. J., & Lane, P. N. J. (2023). Increasing fire frequency may trigger eco-hydrologic divergence. *Hydrological Processes*, *37*(3), e14858. https://doi.org/10.1002/hyp.14858